Hydroconversion of fatty acids and vegetable oils for production of jet fuels

Mäki-Arvela, Päivi; Martínez-Klimov, Mark; Murzin, Dmitry Yu

Published in:
Fuel

DOI:
10.1016/j.fuel.2021.121673

Published: 15/12/2021

Document Version
Final published version

Document License
CC BY-NC-ND

Fuel 306 (2021) 121673

Contents lists available at ScienceDirect

Fuel

journal homepage: www.elsevier.com/locate/fuel

Hydroconversion of fatty acids and vegetable oils for production of jet fuels

Päivi Mäki-Arvela, Mark Martínez-Klimov, Dmitry Yu. Murzin *

Laboratory of Industrial Chemistry and Reaction Engineering, Åbo Akademi University, Turku/Åbo, Finland

ARTICLE INFO

Keywords:
Fatty acids
Oil
Hydroconversion
Jet fuels

ABSTRACT

The review covers transformations of vegetable oils and fatty acids to jet fuel intensively studied during the recent years. A special emphasis is put on the liquid product yields and the product distribution with the latter one affecting the fuel properties. In addition, the desired catalyst properties have been summarized. One of the best results was reported for Jatropha oil processing, giving above 80 wt% yield of the liquid phase products over Ni supported on $H_3PW_{12}O_{40}$/hydroxyapatite at ca. 400 °C under 30 bar hydrogen. Palm oil hydroconversion was performed in a two-step process over Pt/Al_2O_3 followed by Pt/HY, at 395 °C and 245 °C, respectively giving 54% jet fuel components. Typically also other products such as diesel range hydrocarbons are formed. Fatty acid and ester hydroconversion proceeds at lower temperatures, 255–260 °C over Ni supported catalysts producing above 50% yield of the aviation type fuel components. The desired catalyst contains acid sites with weak and medium strength, small metal particle sizes and mesoporosity, which facilitate diffusion of branched alkanes. Reaction kinetics, mechanism and kinetic modelling are also summarized.

1. Introduction

Production methods for renewable jet fuel has attracted a lot of attention both in industry and in academia during the recent years [1–39]. Jet fuels composed mostly of iso-paraffins, n-paraffins, naphthenes, olefins and aromatic components have strictly regulated properties [40]. Aromatic and cyclic components in jet fuels can be produced via pyrolysis [41] and catalytic liquefaction of wood [42,43] giving biocrude. Phenolic compounds in bio-oil can be hydrodeoxygenated and cracked to corresponding cyclic and aromatic compounds [44,45], while algal and vegetable oils, their esters as well as fatty acids and their esters give diesel [14,15], kerosene (C9-C14) [3,17] and naphtha fractions, >C9 hydrocarbons [14], depending on hydroconversion conditions and the type of catalyst. Fatty acids and oils can also be separately deoxygenated, hydroisomerized and hydrocracked to suitable hydrocarbons in the jet fuel range [15,16,21].

Jet fuel has specific strictly defined properties, such as the heating value, viscosity, aromatic content and the desired ratio between the branched to normal alkanes. Its production in one-step can be demanding and thus also multistep methods with several catalysts in different steps have been developed [15,21,31]. Jet fuel production from renewable sources has been very intensively studied during the recent years [12,13,17,20,38], giving, however, depending on the catalyst properties, also diesel [14], gasoline [14] or aromatic [46] fractions.

The aim of this review is to summarize recent literature on hydroupgrading of oils, fatty acids and their esters. Hydroupgrading of oils to produce jet fuels means hydrodeoxygenation, in some cases followed by hydroisomerization and hydroconversion. Some reviews on this topic are already available [47–50]. In [49] bio-jet fuel production from different feedstock is summarized rather broadly with especially the catalyst selection for hydroconversion of acids and esters presented very shortly. In [50] hydroconversion using different feedstock is briefly summarized, without providing any details of catalyst properties. The same holds for Ref. [47], even if the effect of the catalyst support has been discussed in a more detailed manner. The main aim in [48] was to summarize reactor modelling. In the current work, the highest yields of jet fuel components from different feedstock are presented and the desired catalyst properties for production of jet fuel components are discussed in detail including the pore size, acidity, metal dispersion and the catalyst morphology. Furthermore, the effect of different reaction parameters, catalyst stability, kinetics, modelling as well as thermodynamics are summarized. Finally, some recommendations for future research are proposed.

2. Properties of oils and jet fuel

Jet fuels have been produced from different oils including algae, [31], Jatropha, [17,31], soybean [14,23] and palm oil [9], free fatty

* Corresponding author.
E-mail address: dmurzin@abo.fi (D.Yu. Murzin).

https://doi.org/10.1016/j.fuel.2021.121673
Received 26 May 2021; Received in revised form 3 August 2021; Accepted 7 August 2021
Available online 17 August 2021

acids e.g. oleic [12,13] and palmitic [25,27] acids, mixtures of fatty acids [45]. For obvious reasons it is preferable to use non-edible oils as feedstock, e.g. Jatropha oil [14]. Typical fatty acid composition in triglycerides and amounts of free fatty acids in different oils are presented in Table 1.

Jet fuels are composed mostly of iso-paraffins, n-paraffins, naphthenes, olefins and aromatic components [40]. In hydroprocessing of oils more aromatics are formed when high amounts of unsaturated acids, e.g. linoleic and linolenic acids, are present [15]. Typically, the aromatic content is low [16,31], however, some aromatics are required to avoid leaks in seals of the fuel system [40], while olefins are undesired. An acceptable lower level of aromatics according to ASTM D7566 is 8% [20], while in [18] it was pointed out that the optimum amount of aromatic compounds in bio jet fuel is 10–15%. On the other hand, the arene content should be lower than 25% according to ASTM regulations [51]. One of the reasons for such restrictions is a desire to diminish the soot formation.

The heating value (HV) of jet fuels is between 44.5 and 47.3 kJ/g [38,40]. When more aromatics are present the energy density of the fuel is low [7]. The heating value can be calculated from the elemental composition of the jet fuel according to the following formula [38]:

$$\text{HHV (MJ/kg)} = 0.095\cdot S + 1.428\cdot (H\text{-}O/8) + 0.338\cdot C \quad (1)$$

in which S, H, O and C denote the weight percentage of elements in the fuel.

Quality of the jet fuel produced from oils, fatty acids and their esters using heterogeneous catalysts has been reported in a few papers and compared with the ASTM standard (Table 2). Details of the corresponding hydroconversion processes are described in Section 3. Hydroconversion of Jatropha oil (Table 2, entry 3, 4) in one step gave the desired jet fuel properties [17,31]. Sulfur content in the algal oil derived biofuel was analyzed, being below 20 ppm, when hydroconversion was performed using sulfided Ni-Mo-HZSM-5 as a catalyst [31]. One drawback with such catalyst could be formation of S-containing organic compounds in the product [4]. Furthermore, it was possible to produce good quality jet fuel from soybean oil using a three-step method (Table 2, entry 5) [15]. In this method, hydroconversion of soybean oil was performed with Pt/Al_2O_3/SAPO-11 followed by mild hydroconversion of the heavy fraction of the product from the first step over Ni_2P/HY. In the third step isomerization of light naphtha and the jet fraction from step 1 together with the product of step 2 with Pt/Al_2O_3-SAPO-11 gave suitable jet fuel with the desired properties (Table 2, entry 5) [15]. A two-step method, comprising hydrodeoxygenation with 1 wt% Pt/Al_2O_3 and hydroconversion of the product from the first step with 1 wt% Pt/Beta zeolite for production of jet fuel from palm oil was proposed (Table 2, entry 6) [16]. The composition of Jet-A fuel was analyzed in [20] stating that the ratio between isoalkane to linear alkane, I/N ratio of Jet-A was 1.5. The product in hydroconversion of palm oil over NiAg/SAPO-11 exhibited a suitable flash point and an aromatic content (Table 1, entry 7) [20]. The flash point in palm oil derived jet fuel was 38 °C, however, the flash point should be high enough to guarantee fire safety [20,40]. Hydroconversion of methyl palmitate over Ni-BTC-MCM-41 gave good quality jet fuel components with an adequate density and the heating value (Table 2, entry 9) [38].

Cold properties of jet fuel can be described by the freezing point, which decreases for paraffins with decreasing the alkane chain length [4]. A high amount of isoparaffins also decreases the freezing point [16]. The position of the methyl group can also affect the freezing point of isoalkanes, e.g. 5-methylparaffins have a lower freezing point than 2-methylparaffins [4]. A high content of C16 to C18 paraffins in the product is not desired, since otherwise the requirement of freezing point is not met [52], as was the case in the products originating from hydroconversion of microalgae biodiesel in [8] and from refined bleached deodorized palm oil (Table 1, entries 8, 11) [9]. The freezing point of the fuel is directly related to its chemical composition. Acidity of the product from hydroconversion of bleached deodorized palm oil was too high (Table 1, entry 8) [9]. One known method to reduce acidity in petroleum oil is to treat the oil under 0.1 MPa of methanol at 220 °C for 1 h [53], which in general can also be done for biobased jet fuels.

In addition, it has been stated in [2] that bio-based kerosene has some benefits in comparison to petroleum-based fuels, such as low SO_x and particulate emissions due to a lower content of aromatics.

3. Production of jet fuels from oils, fatty acids and esters

Several studies has been made for production of jet fuels from fatty acids, [4,12,13,26,27,36] and esters [35,37,38], microalgae biodiesel [8] as well as from oils, e.g. from Jatropha [1,2,17,31], camelina [21], sunflower [21], palm [9,16,18,20,21,30], coconut [10], soybean [21,23,32], castor [21] and waste cooking oil [5] via hydroconversion, while some publications are concentrating on production of aromatic compounds [45] and diesel-range alkanes [14,32]. It was challenging to summarize the results as there are just few studies in which the yields of different products are given [1,5,9,14,30,31,38] including the gas- [5,13,14,37] and the solid phase products [15]. In fact, in just few studies the mass balance has been determined [3,12]. In some cases also product distribution by groups, e.g. cycloalkanes, aromatic and alkanes [8,35] or by carbon numbers [31,38] or specific products [36] were provided. Several analytical methods, such as two dimensional GC [3,15], GC–MS, [15,22,26] ^{13}C NMR analysis [11] or FTIR [11,22,23] have been utilized for a detailed product analysis. Typically, only the liquid product distribution [20,23,26,27] or selectivity among liquid products [8,13,17,35,37] is reported along with the conversion level, rather that not the absolute yields, as is the case with [6,9,11,12,15,16,22,30,31,32,38]. In Table 3 the most promising results with optimized catalysts and reaction conditions in hydroconversion of oils, acids and ester are given including conversion, yields or selectivity to jet fuel components or alkanes among organic liquid phase products (OLP) and I/N ratio. The proper conditions for producing high-quality jet fuel depend on the feedstock, reaction conditions and selection of the metal and the support. Typically high metal dispersion, large pore sizes or easy accessibility of the reactants to the active sites, e.g. using

Table 1
Chemical composition of different feedstock.

Oil	C20:1	C18:0	C18:1	C18:2	C16:0	C14:0	FFA (%)	Ref.
Jatropha oil	0	7.9	45.4	27.3	19.5	0	1.7	[31]
Palm oil	0.2	3.1	50.1	11.7	24.1	1.6	n.a.	[21]
Soybean oil	5.5	4	29	46	12.5	<3	n.a.	[23]
Sunflower oil	0.3	4.0	24.1	63.7	6.3	0.1	n.a.	[21]
Camelina oil	2.7	2.8	15.0	19.5	5.6	0.1	n.a.	[21]
Castor oil[a]	0	1.0	3.0	5.0	2.0	0	n.a.	[21]
Algal oil		2	39	7	51		1.6	[31]
Maracuja oil	0.2	3.2	11.8	71.4	12.8	0.2	n.a.	[22]
Buriti oil	0	1.3	80.4	0.2	17.1	0.3	n.a.	[22]
Babassu oil	0	3.8	21	1.4	10.8	19.2	n.a.	[22]

[a] 89% ricinoleic acid C18:9-cis(11OH).

Table 2
Jet fuel properties.

Entry	Feedstock	Density at 15 °C	Freezing point (°C)	Boiling point (°C)	Flash point (°C)	Viscosity at −20 °C (mm^2/s)	Heating value (MJ/kg)	Aromatic content ASTM D6379	Acid number (mg KOH/g fuel)	Ref.
1	standard	0.775–0.84	Max. −47	n.a.	Min. 38	Max. 8.0	42.8	8–25 vol%	0.1	ASTM D7566 [15]
2	standard	n.a.	−52- −50	n.a.	n.a.	n.a.	57.25	n.a.	n.a.	[40]
3	Jatropha oil	0.78	−55	n.a.	>38	<8.0	>44	<1	n.a.	[31]
4	Jatropha oil	0.814	−50	n.a.	n.a.	3.75	57.25	n.a.	0.010	[17]
5	Soybean oil	0.776	−50	n.a.	48.5	3.3	n.a.	14.3	0.01	[15]
6	Palm oil	0.763	−48	n.a.	51	7.4	47.1	0	n.a.	[16]
7	Palm oil	n.a.	n.a.	n.a.	58	n.a.	n.a.	9	n.a.	[20]
8	Bleached deodorized palm oil	PRO	–32	n.a.	42	n.a.	45.0	n.a.	14	[9]
9	Methyl palmitate	0.7947	n.a.	n.a.	n.a.	n.a.	45.9	n.a.	n.a.	[38]
10	Methyl palmitate	n.a.	n.a.	n.a.	n.a.	n.a.	47.36	n.a.	n.a.	[35]
11	FAME from nannochloropsis	0.794	−35.54	n.a.	n.a.	6.9 at 5 °C	49.01	n.a.	n.a.	[8]

nanosized supports with intraparticle mesopores and a certain acidity are required. Hydroconversion of oils requires typically higher reaction temperatures (360–410 °C) than that of fatty acids and their esters (250–360 °C). Typically hydrogen pressure for hydroconversion of oils is in the range of 20–50 bar) while hydroconversion of fatty acids and esters is performed under 10–40 bar.

Several catalysts were investigated for Jatropha oil hydroconversion including NiO-MoO_3/Al_2O_3, Pt/SAPO-11 and NiO-MoO_3/H-ZSM-5 (Table 3, entry 1) [31]. Rather harsh conditions are required for hydrotreating of this oil due to its high oxygen content [3]. The highest yield of the jet fuel components, 54% was obtained in a one step process over mesoporous 5 wt% NiO-18 wt% MoO_3/H-ZSM-5 at 410 °C under 50 bar hydrogen [31]. This catalyst gave also products with I/N ratio of 2, which is desired for jet fuel. Based on these initial results it was concluded that a balance between acid sites and hydrogenation-dehydrogenation activity for an efficient catalyst is required. Thus, a mesoporous hierarchical ZSM-5 support was loaded with Ni–W resulting in ca. 40% yield of C9-C14 components. The highest yield of C9-C14 hydrocarbons, 77% in Jatropha oil hydroconversion was obtained over an acidic sulfided 4 wt% NiO-24 wt% WO_3/SiO_2-Al_2O_3 catalyst at 420 °C under 80 bar hydrogen under 0.5 h^{-1} space velocity (Table 3, entry 2) [3]. Pilot experiments were also made with this catalyst at the same temperature giving 30% kerosene, 60% diesel and 12% naphtha products compounds comprising 72% paraffins, 21% cyclic hydrocarbons as well as 7% monoaromatics and 0.1% polyaromatics determined by the two-dimensional GC analysis [3]. Furthermore, 29% of carbon was present in the gas phase.

Hydroupgrading of soybean oil was studied over different catalysts (Table 3, entries 7–10) [15,21,23,32]. The theoretical liquid phase product yield from soybean oil is 81.5%. A rather high yield, 75%, was obtained over 8 wt% Ni/SAPO-11 in [32] while ca. 16% selectivity among all hydrocarbons was observed for C7-C14 hydrocarbons at 370 °C under 40 bar hydrogen (Table 3, entry 9). In a three step process with separate hydrodeoxygenation, hydroconversion and isomerization catalysts 37% yield of jet fuel was obtained (Table 3, entry 8) [15], On the other hand, $NbOPO_4$ gave a high deoxygenation degree, but a low I/N ratio (Table 3, entry 7) [23]. High amounts of aromatic compounds were also formed from soybean oil in its hydroconversion over $NbOPO_4$ at 350 °C under 10 bar hydrogen [23]. It was, however, stated that a too high amount of aromatic compounds can be diminished by increasing a hydrogen pressure. [23] When the mass of $NbOPO_4$ catalyst was increased in hydroprocessing of soybean oil at 350 °C under 10 bar hydrogen, the liquid product distribution changed as well (Fig. 4). The highest amount of hydrocarbons among liquid products was obtained with 25 wt% of the catalyst, while with a lower catalyst amount more intermediate oxygenated species were present in the liquid phase [23]. The isomer to normal alkane ratio calculated for the optimized liquid mixture with 25 wt% of the catalyst was only 0.3 [23], being quite far away from the optimum ratio of 2 for jet fuels giving a high heating value [31].

Analogously to soybean hydroprocessing [15], two step processes were developed for transforming palm oil to jet fuel including in the first step hydrodeoxygenation followed by the second step with an acidic hydroconversion/isomerization catalyst (Table 3, entry 11, 12) [15,16]. Especially in two step process using 1 wt% Pt/Al_2O_3 and 0.5 wt% Pt/HY with SiO_2/Al_2O_3 ratio of 30 as catalysts a high jet fuel yield and a high I/N ratio were obtained (Table 3, entry 11) [15]. It was also stated in [15] that at harsh conditions to be used in hydroconversion of palm oil, the HDO catalyst suffered from sintering and can be easily deactivated, thus a two- step process is proposed. The products in [15,16] did not contain aromatics based on two- dimensional GC analysis. Palm oil hydroconversion to jet fuels was also successfully demonstrated in one-step over NiAg and Pd catalysts under high temperatures and hydrogen pressures (Table 3, entries 12–16) [9,15,16,20,30]. The composition of the liquid phase products obtained from palm oil over 30 wt% NiAg/SAPO-11 at 400 °C under 52 bar hydrogen was close to the one for Jet A-1, while over 1 wt% Pt/SAPO-11 at 450 °C under 59 bar hydrogen the products did not contain enough normal alkanes having with a low heating value. Gaseous products formed from palm oil over 30 wt% NiAg/SAPO-11 were CO, CO_2 and propane. The latter can also be dehydrogenated to propene [20]. Furthermore, the carbon yield in [20] determined as a sum of carbon in liquid, gaseous and solid products was 94%.

Hydroconversion of waste cooking oil, methyl palmitate, algal oil and methyl ester of Nannochloropsis was also successfully demonstrated (Table 3, entries 17–21) [6,8,31,33,37,38]. Noteworthy is the low temperature required for 10 wt% Ni/mesoY to catalyze hydroconversion [8], while other Ni catalysts operated at high temperatures [6,38]. Mesopores were created when the support was treated with an optimum NaOH concentration of 0.4 M. In hydroconversion of algal oil over sulfided 5 wt% Ni-18 wt% MoO_3/H-ZSM-5 (Table 3, entry 21) the conversion increased with increasing temperature while an optimum temperature forming hydrocarbons with the yield of 78% was 410 °C under 50 bar hydrogen [31]. A relatively high selectivity to jet fuel hydrocarbons was obtained in continuous hydroprocessing of fatty acid methyl esters from Nannochloropsis over mesoporous 10 wt% Ni/meso Y containing 4 wt% of Keggin type heteropolyacid at 255 °C under 20 bar hydrogen [8]. Under these conditions ca. 11% arenes were generated with the I/N ratio of ca. 0.8 (Table 3, entry 22).

Oleic and palmitic acid hydroconversion was investigated over Ni-, Mo- and Co-zeolites [4,12,13,26–28,36] and over Ni/Al_2O_3 [13] (Table 3, entries 23–30). Fatty acid hydroconversion occurred over Ni

Table 3
Hydroprocessing of oils, fatty acids and their esters. Notation: Y yield, S selectivity, YF yield fraction among liquid phase products, OLP organic liquid product, AFRA aviation fuel range alkanes.

Entry	Feed	Catalyst	Conditions	Conversion (%)	Yield/Selectivity (%)	I/N	Ref.
1	Jatropha oil	Sulfided 5 wt% NiO-18 wt% MoO_3/H-ZSM-5 (HSAC)	410 °C, 50 bar H_2,	99	Y = 54	2.6	[31]
3	Jatropha oil	Sulfided 4 wt% NiO-24 wt% WO_3/SiO_2-Al_2O_3	420 °C, 80 bar, LHSV = 0.5 h^{-1}	90	$YF=_{C9-C14}$ = 77		[3]
4	Jatropha oil	5 wt% Ni-30 wt% $H_3PW_{12}O_{40}$/nano-hydroxyapatite	360 °C, 30 bar H_2, LHSV = 2 h^{-1}, H_2/oil ratio 600	100	Y_{OLP} = 83.4%	1.64	[11]
5	Jatropha oil	2 wt% Pt/SAPO-11	410 °C, 50 bar H_2, LHSV = 1.2 h^{-1}, H_2/oil ratio 1000 ml/ml	100	S_{C8-C16} = 59%	0.75	[17]
6	Jatropha oil	Sulfided 3 wt% Co 8 wt% Mo/mesoporous titanosilicate (MTS)	360 °C, 80 bar H_2, LHSV = 2 h^{-1}, H_2/oil ratio 1500 ml/ml	80	Y_{C9-C14} = 18%	1.5	[24]
7	Soybean oil	$NbOPO_4$	350 °C, 10 bar H_2, 5 h	Nearly complete conversion	Deox degree 97%, 97% hydrocarbons in liquid phase Y_{OLP} = 62	0.37	[23]
8	Soybean oil	I. 0.5 wt% Pt/Al_2O_3/SAPO-11 II. Ni_2P/HY III. 0.5 wt% Pt/Al_2O_3-SAPO-11	I. 370 °C, 30 bar H_2, LHSV = 1 h^{-1} II. 315 °C, 30 bar H_2, 4–7 h^{-1} III. 350 °C, 30 bar H_2, LHSV = 2–4 h^{-1}		$Y_{jet\ fuel}$ = 37 wt%		[21]
9	Soybean oil	8 wt% Ni/SAPO-11	370 °C, 40 bar H_2, LHSV = 1 h^{-1}	100	Y_{OLP} = 75 S_{C7-C14} = 16	85% isomers	[32]
10	Soybean oil	sulfided 2.7 wt% Ni-12.7 wt% Mo/γ-Al_2O_3	360 °C, 140 bar H_2, 8 h		Y_{OLP} = 70.9		[22]
11	Palm oil	I. 1 wt% Pt/γ - Al_2O_3, II: 1 wt% Pt/nano-beta zeolite	360 °C, 20 bar H_2, II. 235 °C, 20 bar H_2, 5 h III. distillation		Y = 54.8 wt%	7.0	[16]
12	Palm oil	I. 1 wt% Pt/γ-Al_2O_3, II: 0.5 wt% Pt/HY (SiO_2/Al_2O_3 = 30)	I. 395 °C, 40 bar H_2, II. 245 °C, 50 bar H_2, WHSV = 2 h^{-1}		Y_{OLP} = 81.6 wt% S_{C8-C16} = 66.1 wt%	4.67	[15]
13	Palm oil	30 wt% meso NiAg/SAPO-11	400 °C, 52 bar H_2, LHSV = 1 h^{-1}	100	S_{C8-C16} = 84%	2.1	[20]
14	Palm oil	10 wt% Ni/SAPO-34	390 °C, 52 bar H_2, 8 h	97	Y_{C8-C16} = 41[b]		[18]
15	Palm oil	0.5 wt% Pd/Al_2O_3	400 °C, 60 bar H_2, 2 h		$Y_{kerosene}$ = 43% Y_{diesel} = 50%[c]		[30]
16	Bleached deodorized palm oil	0.5 wt% Pd/Al_2O_3	477 °C, 56 bar H_2, LHSV = 1.5 h^{-1}		$Y_{kerosene}$ = 48%[c]		[9]
17	Waste cooking oil	25 wt% Ni- 0.5 wt% Ag/SAPO-11	380 °C, 40 bar H_2, WHSV = 2 h^{-1}	72	S_{C8-C16} = 40[d]	1.23	[6]
18	Waste cooking oil	Presulfided 4 wt% Ni-12 wt% Mo/USY	380 °C, 30 bar H_2,		S = 42%		[33]
19	Methyl palmitate	10 wt% Ni/meso-Y	390 °C, 20 bar H_2,	91	S = 64.8	0.3	[37]
20	Methyl palmitate	2.5 wt% Ni-BTC-MCM-41	390 °C, 20 bar H_2, 6 h	n.a.	Y = 53.2%	n.a.	[38]
21	Algae oil	Sulfided 5 wt% NiO-18 wt% MoO_3/H-ZSM-5 prepared in the presence of (ODAC)[e]	410 °C, 50 bar H_2	98	Y_{OLP} = 78.5	2.5	[31]
22	FAMe from Nannochloropsis	10 wt% Ni/meso Y-HPW	255 °C, 20 bar H_2,	97.2	$Y_{jet\ biofuel}$ = 63.1	0.8	[8]
23	Oleic acid	10 wt% Ni-ZSM-5 nanosheet	250 °C, 10 bar H_2,		S_{AFRA} = 51.4	1.7	[12]
24	Oleic acid	4 wt% Ni/Al_2O_3 ALD	360 °C, 30 bar H_2, WHSV = 2.4 h^{-1}, cylohexane as a sovlent	100	S_{AFRA} = 37.2	2.7	[13]
25	Oleic acid	10 wt% Ni/ZSM-5 nanosheet	250 °C, 10 bar H_2, WHSV = 2.4 h^{-1}, cylohexane as a sovlent	100	S_{AFRA} = 51.4	1.7	[12]
26	Palmitic acid	4.4 wt% Ni-HMP-49	260 °C, 40 bar H_2, 4 h, decalin as a solvent	>99	$S_{C12-C14}$ = 53.5[a]	0.9	[28]
27	Palmitic acid	4 wt% Ni-H-ZSM-22 (5 wt% NiO)	260 °C, 40 bar H_2	100	$S_{C14-C15}$ = 73.8[a]		[4]
28	Palmitic acid	5 wt% CoO over desilicated H-MCM-49	260 °C, 40 bar H_2, 4 h, n-decane as a solvent	>99.9	S_{12-14} = 29.3	0.5	[26]
29	Palmitic acid	21 wt% Mo/H-ZSM-22	260 °C, 40 bar H_2, 4 h	82	S = 61.7% isoalkanes		[36]
30	Palmitic acid	5 wt% Co-HZM-5	260 °C, 40 bar H_2, 4 h, n-decane	100	$S_{C13-C16}$ = 100%	0.51	[27]

[a] among liquid phase product, [b] mass based yield.
[c] determined by volume fraction obtained via distillation, [d] selectivity among C1-C18 alkanes, except for C15-C18.
[e] ODAC denotes octadecyldimethyl-(3-trimethoxysilylpropyl)ammonium chloride.

supported zeolites at lower temperatures in comparison to e.g. soybean oil hydroconversion [32]. For oleic acid the yield of the aviation fuel range alkanes (AFRA) was ca. 51% with 97% carbon balance at 250 °C under 10 bar hydrogen over 10 wt% Ni/ZSM-5 nanosheet catalyst (Table 3, entry 23) [12]. Jet fuel range alkanes could be produced from palmitic acid over 4 wt% Ni-HMP-49 prepared from post-synthesizing H-MCM-49 with tetraethylammonium hydroxide and melt infiltrating nickel on it [28] (Table 3 entry 26, Table S1, entry 26). The reaction conditions were 260 °C and 40 bar hydrogen and after 4 h 100% selectivity to alkanes was obtained. This product contained ca. 49% C_{12}-

C_{14} cracking compounds with the ratio I/N of 0.9. Analogously mesoporous, post-treated 5 wt% CoO/H-MCM-49, was efficient in hydroupgrading of palmitic acid (Table 3, entry 28, Fig. 2) [26]. The desired catalyst properties for production of the jet fuels from fatty acids and oils are an appropriate pore size, the presence of strong acid sites facilitating hydroisomerization and hydrocracking [28].

Cycloalkane formation was investigated in hydroconversion of model fatty acids, i.e. stearic, oleic, linoleic and linolenic acids over sulfided 2.7 wt% Ni-12.7 wt% Mo/γ-Al_2O_3 catalyst at 360 °C under 140 bar hydrogen for 2 h. The main products were n-$C_{17}H_{36}$ and $C_{18}H_{38}$, while also large amounts of cycloalkanes were formed, especially when using linolenic acid as a feedstock [22].

In addition to cycloalkanes also alkylbenzenes, such as heptyl benzene, 2-methyloctylbenzene, dodecyl benzene, were formed in ca. 7 wt% from linolenic acid (Fig. 3). Formation of aromatic products in hydroconversion of oils over 1 wt% Pt/Al_2O_3/SAPO-11 depends on the amount of polyunsaturated fatty acids in the feedstock. It can be concluded from Fig. 3 that palm and tallow oils are hydrogenated, while more aromatic compounds are formed from soybean, sunflower and camelina oils [21].

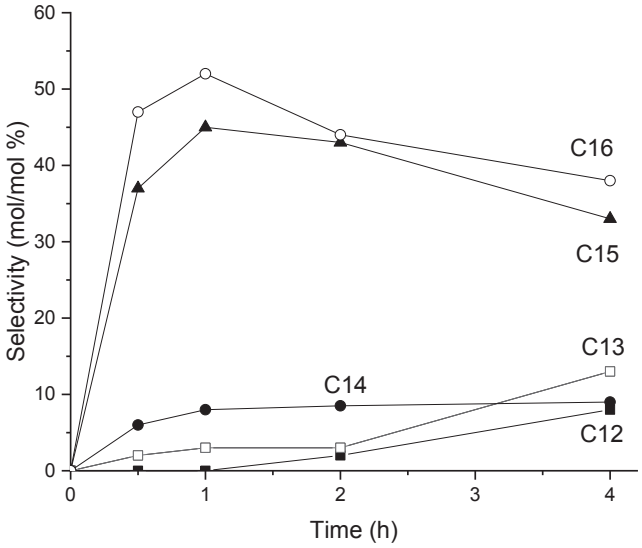

Fig. 2. Selectivity for liquid phase products in hydroconversion of palmitic acid over 5 wt% CoO on desilicated HMCM-49 at 260 °C under 40 bar hydrogen in n-decane as a solvent,
adapted from [26]

4. Catalyst selection

The product properties in hydroprocessing of oils, fatty acids and their esters over different catalysts depend on the type of feedstock, reaction conditions as well as on the catalyst properties. For production of jet fuels by hydroconversion of fatty acids and oils, bifunctional catalysts with the metal and acid functions are needed, in which the metal facilitates hydrogenation/dehydrogenation and hydroconversion, while acidity is needed for cracking and isomerization. Metal modified zeolites exhibit high acidity, with the disadvantage that, their pores sizes are below 0.7 nm. Triglycerides are large molecules with a cross-section of ca. 0.6 nm [20], therefore configurational diffusion of the reactants and products inside the catalyst pores is also very important. Because a high I/N ratio is a desired property in jet fuels, the sizes of isomers should considered in relation to the pore sizes. The sizes of n-paraffins, monobranched, dibranched and tribranched isomers have been approximated as 0.45 nm, 0.58–0.6 nm, 0.61–0.63 nm and 0.65 nm, respectively [54] showing clearly that the zeolites can experience mass transfer limitations. The parameters, which can be fine-tuned for the production of jet fuel are the metal type and particle size, reducibility of the metal, as well as acidity of the catalyst. From the viewpoint of catalyst morphology mesoporosity [15,17,20,23,31,33,38] is beneficial or alternatively nanosized catalyst particles are applied [16,38] (Table 3). Several alternatives exist to create mesoporosity and promote accessibility to the active sites, such as utilization of mesoporous supports (MCM-41), desilication by NaOH treatment [33,37] and dealumination of zeolites [31,33], formation of mesoporous pellets, application of surfactants and different ratios of meso- micropore structural directing agents [31] or utilization of zeolite nanosheets [12,16]. In addition, structured mesoporous catalysts, such as Ni-mesoporous organic framework modified MCM-41, have an opportunity to limit arene formation from methyl palmitate hydroconversion [38].

Supports with suitable properties, such as mesoporosity, as well as appropriate acidity which can be tuned with additives, such as

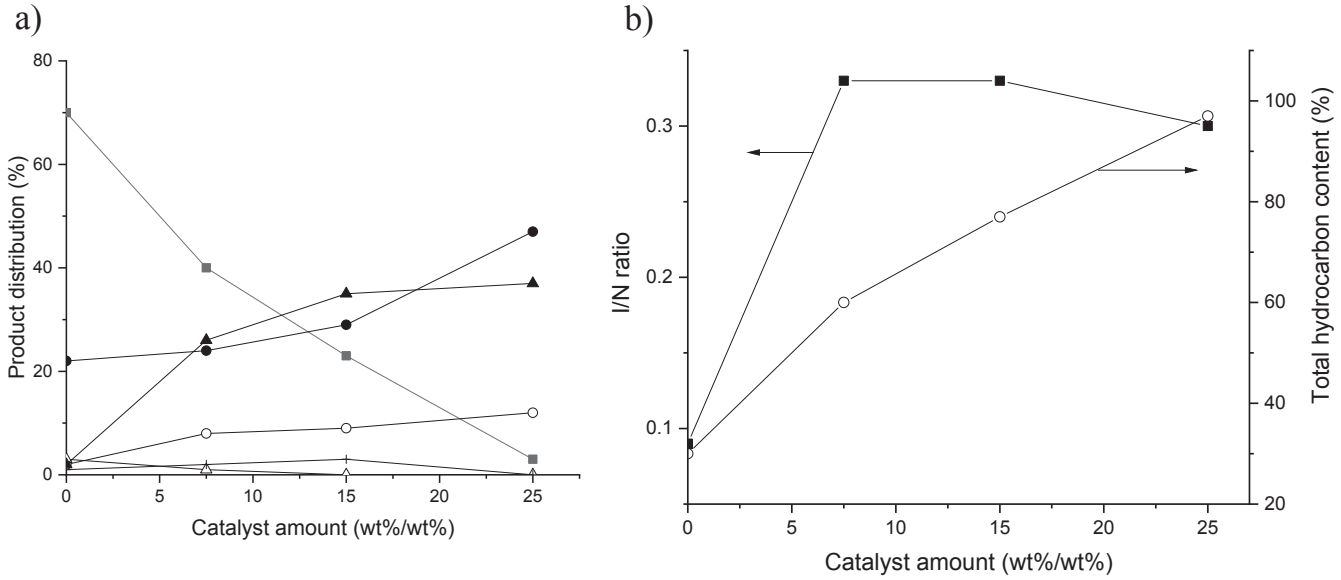

Fig. 1. a) Product distribution in hydroconversion of soybean oil over $NbOPO_4$ under 10 bar hydrogen at 350 °C in 5 h. Notation: (■) oxygenated products, (▲) aromatics, (●) alkanes, (o) isoalkanes, (+) cycloalkanes and (Δ) olefins, b) (■) I/N ratio and (o) the total content of hydrocarbons .
adapted from [23]

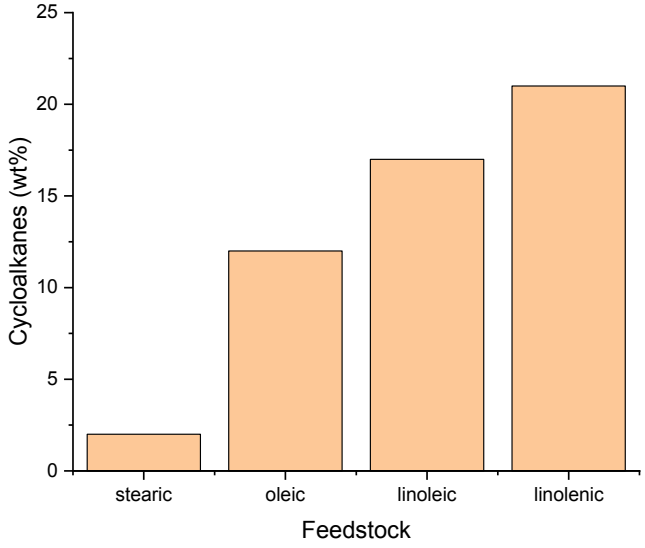

Fig. 3. The amount of formed cycloalkanes in hydroconversion of fatty acid at 360 °C under 140 bar for 2 h over sulfided 2.7 wt% Ni-12.7 wt% Mo/γ-Al_2O_3, adapted from [22]

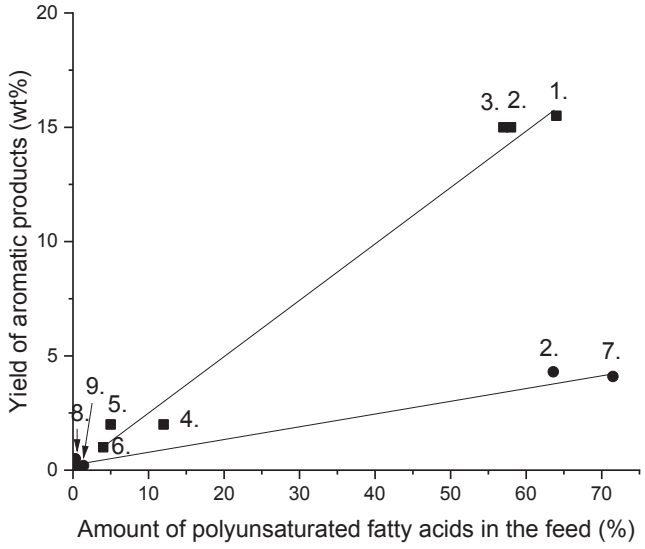

Fig. 4. The yield of aromatic products as a function of the amount of unsaturated fatty acids in the feed in hydroprocessing of different oils over a) 1 wt% Pt/Al_2O_3/SAPO-11 at 370 °C under 30 bar hydrogen adapted from [21] (■) and b) sulfided 2.7 wt% Ni-12.7 wt% Mo/γ-Al_2O_3 at 360 °C under 140 bar hydrogen adapted from [22] (●). Notation: 1. sunflower, 2. soybean, 3. Camelina, 4. palm, 5. castor, 6. tallow, 7. Maracuja, 8. Babassu and 9. Buriti oil.

phosphotungstic acid [8,11] or by adding a second metal, such as silver [5], are beneficial for a proper hydroconversion catalyst. Acidity can also be tuned via the post-synthesis, e.g. dealumination and desilication, which also creates mesopores as mentioned above. In some cases, acidity can also be too high and it can be decreased by the silane treatment [12]. Mesoporosity is often correlated with high acidity [20] and a high metal dispersion [17] as can be seen from Table 4.

Metal selection is also crucial, with noble metal catalysts being more expensive, at the same time facilitating use of milder reaction conditions than with transition metal catalysts. A metal should be highly dispersed on the support and its better reducibility typically enhances catalyst performance. In some cases even the oxidation state of the metal oxide is crucial, for example with Mo/H-ZSM-22, when the ratio Mo^{4+}/Mo^0 played an important role [36]. In bimetallic catalysts the electron transfer effect between the two metals can enhance metal reducibility, for example between Ni and W [11]. Thus Ni-$H_3PW_{12}O_{40}$/hydroxyapatite was efficient for hydroconversion of Jatropha oil [11]. In addition, the nature of the two metals over the same support, for example mesoporous titanosilicate was studied and a large difference in the performance of Ni-Mo vs Co-Mo supported on mesoporous titanosilicate was observed [24] and will be discussed below.

In this chapter catalyst performance – property relationship will be discussed, especially elucidating the metal particle sizes, catalyst morphology, optimum reaction conditions for specific catalysts and the product quality obtained in hydroconversion of fatty acids, esters and oils.

Table 4
The properties of the most promising catalysts used in hydroprocessing of oils, fatty acids and their esters.

Entry	catalyst	D pore (nm)	Total acidity (mmol NH_3/g)	Dmetal (nm)	Ref.
1	2 wt% Pt-SAPO-11	3.5	n.a.	11.2	[17]
2	I. Pt/γ-Al_2O_3, II: 1 wt% Pt/nano-beta zeolite	n.a	[a]	1–2	[16]
3	0.95 wt% Pt/Al_2O_3	21–24	0.132 (Lewis acidity)	1.2	[15]
4	1 wt% Pt/Al_2O_3/SAPO-11	3.7	n.a.	7	[21]
5	4 wt% Ni/Al_2O_3	n.a.	0.604	3.1	[13]
6	4 wt% Ni-H-ZSM-22	n.a	n.a.	13–66	[4]
7	10 wt% Ni-SAPO-34	n.a.	n.a.	n.s.	[18]
8	8 wt% Ni/SAPO-11	n.a.	1.84.	n.a.	[32]
9	10 wt% Ni/meso-Y	2–10	n.a.	14–17	[37]
10	4.4 wt% Ni-HMCM-49 post-treated	n.a.	n.a.	20–40	[28]
11	2.5 wt% Ni-BTC-MCM-41 nanosheets	3.7	n.a.	2–8	[38]
12	10 wt% Ni/ZSM-5 nanosheets	9.8	n.a.	10	[12]
13	5 wt% Ni/H-ZSM-5	n.a.	n.a.	10–60	[27]
14	25 wt% Ni- 0.5 wt% Ag/SAPO-11	n.a.	n.a.	n.a.	[5]
15	30 wt% meso NiAg/SAPO-11	5.8	n.a.	4–6	[20]
16	Sulfided 4 wt% NiO-24 wt % WO_3/SiO_2-Al_2O_3	4.6	1.1	n.a.	[3]
17	Ni-Mo/H-ZSM-5 (5 wt% NiO, 18 wt% MoO_3) (high surface area catalyst, HSAC)	3.8	0.42	n.a.	[31]
18	10 wt% Ni/MCM-41 + 20 wt% HPW	3.46	0.73	n.a	[35]
19	10 wt% Ni/Y −4 wt% $H_3PW_{12}O_{40}$	2	n.a.	n.a.	[8]
20	5 wt% Ni-30 wt% $H_3PW_{12}O_{40}$/nano-hydroxyapatite	19.4	n.a	n.a.	[11]
21	5 wt% CoO in Co-HMCM-49P	[b]	[b]	<5	[26]
22	21.2 wt% Mo/H-ZSM-22	[c]	[c]	7–8	[36]
23	3 wt% Co-8 wt% Mo /mesoporous titanosilicate	3.2–3.5	0.5	n.a.	[24]
24	$NbOPO_4$	4–6	n.a.	n.a.	[23]

[a] Total acidity by pyridine adsorption–desorption FTIR for Pt nano Beta zeolite 401 μmol/$g_{cat,}$ [b] no mesopores, total acidity by pyridine adsorption–desorption FTIR at 250 °C for the support 845 μmol/$g_{cat,,}$ [c] micropores, large amount of acid sites with weak and medium strength

4.1. Pt catalysts

Several different types of catalysts have been used in hydroconversion of fatty acids and oils, such as noble metal catalysts (Table 4, entries 1–4) as well as less expensive transition metal catalysts (Table 4, entries 5–24).

In hydroconversion of vegetable oils, Pt was supported both on a moderate acidic SAPO-11 [17] as well as on a composite Al_2O_3/SAPO-11 [21]. Because the metal dispersion is important to get a high hydroconversion efficiency [17], in the former case of Pt/SAPO-11 dispersion of platinum was boosted via using sodium dodecyl benzene sulfonate as a surfactant. In that case Pt particles of ca. 11 nm were obtained. Furthermore, this support exhibited a larger pore size in comparison to the parent SAPO-11 with such larger pore sizes of 2 wt% Pt/SAPO-11 being important for production of jet fuel components from Jatropha oil [17]. The catalyst exhibited a higher specific surface area and the pore size, i.e. 206 m^2/g and 3.5 nm, respectively, than its counterpart prepared in the absence of a surfactant, namely 195 m^2/g and 3.2 nm (Table 4, entry 1, Table S1, entry 1) [17]. For Pt/SAPO-11 with and without the surfactant the jet fuel yields from Jatropha oil were 59% and 45%, respectively at 400 °C under 50 bar hydrogen. Furthermore, more C8-C16 isomers were generated over the former catalyst, e.g. 25% in comparison 21% over Pt/SAPO-11 prepared without the surfactant. Acidity of the catalysts was not determined. In addition, micro-mesoporous Pt/SAPO-11 gave also a high yield of jet fuel components from Jatropha oil (54%). It was concluded in [31] that mesoporosity is necessary to obtain a high and stable catalyst performance. In [17] hydrotreating of different vegetable oils was performed using Pt/Al_2O_3/SAPO-11 composite catalyst. Hydrodeoxygenation of soybean oil was successfully performed over this catalysts giving>60% isoparaffinic compounds (See Section 3). This catalyst exhibited also mesopores and relatively small Pt size size (Table 4, entry 4).

Nanosize support particles have also been tested as metal supports for hydroconverison of vegetable oils [16]. They exhibit intercrystalline mesoporosity enhancing thereby mass transfer. Furthermore, it is easier to achieve a better metal dispersion on nanosized support particles and enhance metal reducibility as well as to optimize acidity. Because Pt/Al_2O_3 is an efficient catalyst for generating long chain hydrocarbons from palm oil [16], not being efficient for producing jet fuel, a two step process was developed in which the long chain hydrocarbons were produced in the first step over Pt/Al_2O_3 and the product was used as a feedstock for jet fuel generation with bulk and nanosized Pt catalysts supported on ZSM-5 and Beta. A comparative work using both Pt supported on bulk and nano sized particles was performed in hydroconversion of long chain hydrocarbons produced from palm oil in [16]. Nanosized Beta particles exhibited sponge like morphologies with the size of 10 – 50 nm and intercrystalline mesoporosity, while the crystallite size of bulk Beta zeolites was>100 nm. The ratio between the surface Pt to the Brønsted acid sites was demonstrated to influence the yield of jet fuel components and I/N ratio (Fig. 5), showing that Pt supported on both bulk and nano Beta zeolite gave a higher I/N ratio to Y_{C8}-Y_{C16} ratio in comparison to Pt-ZSM-5 catalysts. For both Beta and ZSM-5 the nanosize catalysts exhibited a slightly better performance than the corresponding bulk catalysts. At the same time, the latter catalysts exhibited a lower n_{Pt}/n_{BA} ratio in comparison to the nano sized catalysts. The lowest ratio of the mesoporous to the microporous volume was also determined for Pt/nano-Beta, which gave the highest yield of jet fuel hydrocarbons.

Diffusion kinetics was investigated in [16] using 2,2,4-trimethylpentane as a model compound at room temperature for different Pt catalysts supported on bulk and nano Beta and ZSM-5 [16]. Diffusion kinetics was analyzed with the Fick second diffusion law

$$\frac{\partial C}{\partial t} = D\left(\frac{\partial^2 C}{\partial x^2}\right) \tag{2}$$

in which C is the concentration, D is diffusivity, t time and × location. The crystal shape was regarded as the slab-like when the normalized uptake q(t)/q(∞) is defined as

$$A = \frac{q(t)}{q(\infty)} = \frac{2}{\sqrt{\pi}}\sqrt{\frac{D}{L^2}}\sqrt{t} \tag{3}$$

in which L is the characteristic diffusion path length.

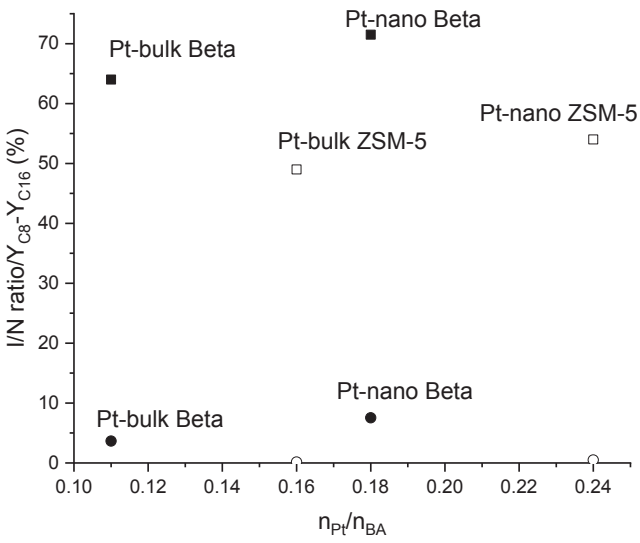

Fig. 5. Correlation between C8-C16 yield to I/N paraffin ratio in hydroconversion of palm oil at 235 °C under 20 bar hydrogen with D/L^2 of 2,2,4-trimethylpentane for different catalysts, adapted from [16]. Open symbol denotes Pt-ZSM-5 catalysts and solid one Pt-Beta catalysts.

When diffusivity divided by the characteristic diffusion path length of each catalyst was correlated with the obtained maximum yield of C8-C16 hydrocarbons and the I/N ratio over the same catalysts, it was concluded that both parameters in hydroconversion of palm oil over different Pt catalysts increased with increasing the diffusion rate [16]. In [16] it was also concluded that the highest yield of the desired products was obtained with nanocrystalline Pt/Beta zeolite catalyst with the highest molecular diffusion rate (Fig. 6). Slower diffusion rates result in over-cracking.

Analogously to [16], easy diffusion of reactants and products was facilitated by mesoporosity in 1 wt% Pt/Al_2O_3/SAPO-11 extrudates of unspecified acidity, which were used in hydroconversion of different oils. The suitable mesopore size was 3.7 nm and Pt was uniformly distributed inside the pellets (Table 4, entry 4) [21].

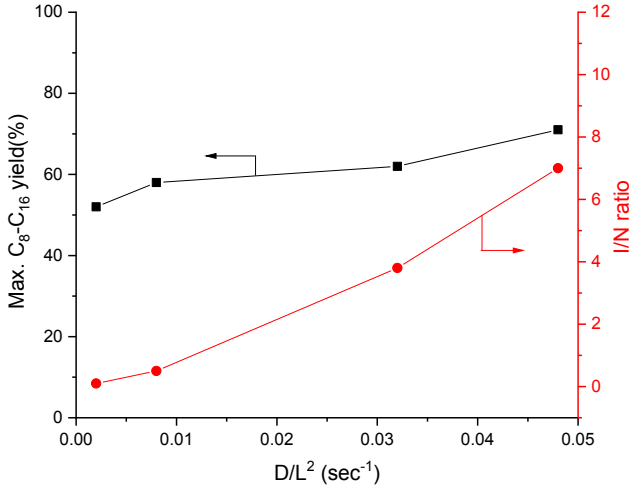

Fig. 6. Yield of C8-C16 hydrocarbons (rectangular) and I/N ratio (ball) in hydroconversion of palm oil at 235 °C under 20 bar hydrogen with LHSV of 2 h^{-1} over different Pt catalysts as a function of the ratio between surface Pt to amount of Brønsted acid sites adapted from [16]. Notation: solid symbols: Pt-Beta catalysts and open symbols: Pt-ZSM-5 catalysts. BA - amount of Brønsted acid sites.

4.2. Ni catalysts

Several inexpensive nickel supported catalysts e.g. monometallic [4,12,13,28,35,38] and bimetallic Ni [1,3,20,31,34], have been applied in hydroprocessing of oils and fatty acids to produce aviation fuel range components. In addition, Ni catalysts combined with phosphotungstic acid have been efficient catalysts for production of jet fuels (Table 4, entries 18–20) [8,11,35].

4.2.1. Monometallic Ni catalysts

For monometallic Ni catalysts the jet fuel production was promoted using highly dispersed Ni particles and suitable acidity [4,13]. Specific catalyst preparation methods, such as atomic layer deposition [13] and melt impregnation were used to enhance the desired catalyst properties for production of jet fuel components, e.g. metal dispersion [4] and metal reduction [4] as well as acidity [4] in comparison to the catalysts prepared by incipient wetness method. In such cases Ni/Al_2O_3 was prepared by the atomic layer deposition [13] while 5 wt% NiO/H-ZSM-5 was synthesized by the melt impregnation [4].

Catalyst morphology was also an important parameter [13,38]. For example, mesoporosity in zeolites [33,37] and the mesoporous materials, e.g. MCM-41 as well as nanosizes ZSM-5 [12] and MCM-41 nanosheets [38] was suitable for their application as supports. The desired properties are high metal dispersion [13], suitable acidity [12,38] and a high diffusion rate [37]. In addition, Ni supported on SAPO-34 was efficient producing only a small amount of arenes [18].

The catalyst preparation method can also affect the metal dispersion [4] and the type of metal sites [13]. It is known that, for example, the atomic layer deposition [13] and the melt infiltration method [4,26] increase the metal dispersion. A comparative work in oleic acid hydroconversion was performed with 4 wt% Ni/Al_2O_3 prepared by atomic layer deposition (ALE) and incipient wetness (IW) methods [13]. The former has only Lewis sites and the particle size smaller in comparison to the one prepared by the incipient wetness method, being 3.6 nm and 6.1 nm, respectively. Furthermore, structure sensitivity in oleic acid hydroconversion was confirmed [13]. 4 wt% Ni/Al_2O_3 ALD contained only Lewis acidic sites. A higher alkane selectivity was obtained over 4 wt% Ni/Al_2O_3 ALD in comparison to the catalyst prepared by the incipient wetness method. It was stated that 4 wt% Ni/Al_2O_3 prepared by ALD contained a higher amount of Ni step sites, which was confirmed by CO TPD, showing presence of a peak above 450 °C, ascribed to associative adsorption of CO on Ni step sites [55]. As acidity and porosity of the catalysts were similar, a better performance of Ni/Al_2O_3 ALD in comparison to Ni/Al_2O_3 IW was correlated with the higher amount of Ni step sites facilitating C–C, C–O and H–H cleavage [55].

A higher Ni dispersion was obtained when the melt infiltration method was applied, as in the case of 4 wt% Ni supported on HZSM-22 (Table 4, entry 6) [4]. Three different methods, melt infiltration, incipient wetness and wetness impregnation [4] were used for preparation of 4 wt% Ni supported on HZSM-22. In the melt infiltration method the dried support was in contact with $Ni(NO_3)_2{\cdot}6H_2O$ at 65 °C for 24 h [56]. This synthesis temperature is above the melting point of the Ni precursor which is impregnated by the capillary forces into the zeolite pores. 4 wt% Ni/HZSM-22 prepared by the infiltration method exhibited also the highest hydrogen consumption in hydrogen TPR and was more active towards formation of isoalkanes in palmitic acid hydroconversion [4]. Strong acid sites promote formation of branched alkanes from palmitic acid [4]. Formation of iso-alkanes was promoted by a higher Ni dispersion on an acidic support, such as on 4 wt% Ni-H-ZSM-22 prepared by the melt infiltration method with Si/Al ratio of 37.5, a high surface area, high crystallinity and a rather high Ni dispersion.

Ni-loading in Ni-BTC/MCM-41 (BTC denotes 1,3,5-benzene-tricarboxylate metal organic framework) catalyst was varied in the range of 2.5 – 20 wt% [38]. Among the studied catalysts, the best one giving a high amount of jet fuels but a low content of aromatic products was 2.5 wt% Ni-BTC/MCM-41 (Table 4, entry 10). These catalysts were prepared as follows: Ni-1,3,5-benzenetricarboxylate metal organic framework (MOF) was synthesized according to [57]. In this method MCM-41 was added into the synthesis solution of MOF and the synthesis was performed at 150 °C for 12 [38]. Thereafter, the catalyst was calcined in air at 550 °C for 4 h. According to EDS mapping Ni-BTC was uniformly loaded inside the pores of MCM-41 [38]. Mesoporous 2.5 wt% Ni in the metal organic framework BTC supported on MCM-41 exhibited a suitable pore diameter of 3.7 nm (Table 4, entry 11), which could partially hinder aromatization, while the pore size of ca. 4 nm nm in 10 wt% Ni in BTC/MCM-41 promoted formation of aromatic compounds in methyl palmitate hydroconversion [38]. Furthermore the best catalyst exhibited more Ni^{2+} than the corresponding 10 wt% Ni catalyst which can be explained by elevation of hydrodeoxygenation ability with a higher content of Ni^{2+} related to more reactive electrons in its unsaturated *d* orbitals [37]. In addition, weak acidity of 2.5 wt% Ni-BTC-MCM-41 based on the peak at 420 °C in ammonia TPD was qualitatively confirmed to be much higher than that for 10 wt% Ni-MCM-41. Besides weak acidity, 2.5 wt% Ni-BTC-MCM-41 exhibited also a small amount of strong acid sites desorbing ammonia at 575 °C [38]. As a comparison 10 wt% Ni-MCM-41 possessed 20 nm Ni particles on MCM-41, when Ni-MOF was not used showing that it was difficult to efficiently disperse nickel on MCM-41. It was also concluded in [38] that the use of Ni containing metal organic framework modified with mesoporous MCM-41 can decrease Ni consumption by 75% still affording a better catalytic performance than 10 wt% Ni/MCM-41 catalyst, These results indicate that such type of novel catalysts has a potential in hydroconversion of fatty acid esters. Furthermore, a low arene content was obtained in the liquid product due to a beneficial catalyst morphology.

Performance of different Ni catalysts supported on MCM-41, HY, SAPO-11 and H-Beta was investigated in palm oil hydroconversion at 390 °C under 30 bar hydrogen [18]. 10 wt% Ni supported catalysts (MCM-41, HY, SAPO-11 and H-Beta) were prepared by wet impregnation in water and dried, calcined and reduced at 500 °C for 4 h. The most important factor determining the yield of the jet fuel components was acidity. In particular 10 wt% Ni/SAPO-34 exhibited the highest alkane and the lowest arene selectivity in hydroconversion of palm oil. Ammonia TPD was qualitatively discussed showing that the best catalyst, Ni-SAPO-34, exhibited the second highest amount of weak acid sites (Table 4, entry 7), while Ni/HY was the most acidic. 10 wt% Ni/H-Beta and Ni/MCM-41 possessed more medium strong acid sites. Among arene products also polycyclic arenes were formed in high amounts over Ni-H-Beta, HY, SAPO-11 and MCM-41 [18].

Desilication with alkali is one method to produce mesopores. 10 wt% Ni supported on mesoporous Y zeolite was prepared by loading nickel with the wet impregnation method (Table 4, entry 9, Table S1, entry 9). For desilication of Y zeolite different amounts of NaOH were used [37] and the highest specific surface area was obtained for Ni/meso-Y catalyst desilicated with an optimum amount of NaOH, namely 0.4 M. This catalyst contained also a large amount of mesopores in the range of 2–10 nm, which was favorable for mass transfer during hydroconversion of methyl palmitate and promoted formation of jet fuel components. With a too high NaOH amount, 0.8 M, the zeolite framework was partially destroyed. When using an optimum NaOH for desilication, some defects emerged and at the same time an increased acid intensity was obtained when some silicon atoms were removed.

In order to enhance mass transfer properties in acidic zeolites, 10 wt % Ni loaded on nanosheet ZSM-5 was also prepared and tested in oleic acid hydroconversion at 250 °C [12]. Since acidity of ZSM-5 is very high, Ni/ZSM-5 nanosheet catalysts were treated with tetraethoxysilane by a chemical liquid deposition method (CLD) to tune the acidity of the catalyst (Table S1, entry 12). The ZSM-5 nanosheets were prepared in one-step hydrothermal process using the Gemini-type quaternary ammonium surfactant ($C_{22}H_{45}$-$N^+(CH_3)_2$)-C_6H_{12}-$N^+(CH_3)_2$-C_6H_{13}) as a structure- directing agent. By using TEOS modified nanosheet in 10 wt% Ni/ZSM-5 the amount of external Brønsted acid sites decreased with an

increasing Si/Al ratio. When the amount of external Brønsted acid sites, determined from pyridine FTIR with 2,6-di tert butyl pyridine, increased, turnover frequency and the I/N ratio of the product also increased in oleic acid hydroconversion (Table 4, entry 12) [12]. An optimum amount of external Brønsted acid sites was found in 10 wt% Ni/ZSM-5 nanosheets with Si/Al ratio of 200, which was treated once with silane and gave a rather high I/N ratio, but not too high ratio of (C4-C8)/(C10-C14) [12]. It was concluded in [12], that a low amount of external Brønsted acid sites promoted primary cracking, while too high acidity enhanced undesired secondary cracking.

4.2.1.1 Bimetallic Ni catalysts

Several bimetallic Ni catalysts have also been tested in hydroconversion of fatty acids and oils [5,20,24,31]. Another metal can have several roles, such as inhibiting extensive cracking [5] or enhance reducibility of metals [11,35]. For example, a bimetallic 30 wt% NiAg/SAPO-11 catalyst with a relatively high Ni dispersion was an efficient catalyst in palm oil hydroconversion [20]. This catalyst was prepared in the presence of citric acid as a chelating agent (Table 4, entry 15, Table S1, entry 15) [58,59], which can increase Ni dispersion, as was demonstrated in [20]. Furthermore, the role of Ag in 25 wt% Ni- 0.5 wt % Ag/SAPO-11 was to inhibit too extensive cracking [5]. The specific surface area of 30 wt% NiAgSAPO-11, which was prepared in the presence of citric acid was the same for the parent SAPO-11 [20], while acidity of NiAg/SAPO-11, being only qualitatively investigated with pyridine FTIR, was, especially Lewis acidity, ascribed to removal of Al from the framework sites [62]. In palm oil hydroprocessing over Ni-Ag/SAPO higher I/N ratios were obtained with the catalyst prepared in the presence of citric acid than over the counterpart synthesized without citric acid addition. The origin for a better performance of the former catalyst is related to its mesoporosity, a higher Ni dispersion and removal of Al from the framework with the citric acid treatment which increased Lewis acid concentration [60].

Sulfided mesoporous 4 wt% NiO-24 wt% WO_3/SiO_2-Al_2O_3 pellets were efficient in generating C_9-C_{14} compounds from Jatropha oil at long residence times and 420 °C (Table 4, entry 16) [3]. Ni was loaded on the pellets by the incipient wetness method. This catalyst was highly acidic, however, out of total acid sites, 71% were weak ones as the desorption peak was found below 330 °C. The ratio between the Lewis to Brønsted sites determined by DRIFTs was 0.56. Furthermore, the large pore size of 4.6 nm promoted formation of the jet fuel components. It was concluded in [2] that if the catalyst has a high hydrogenation ability, less waxy products are formed.

The pore size of hierarchical 5 wt% NiO-18 wt% MoO_3/H-ZSM-5 was varied using different ratios of micro- to mesoporous structural directing agents (Table 4, entry 17) [31]. 5 wt% NiO 18% MoO_3/H-ZSM-5 was presulfided with dimethylsulfide to transfer the inactive oxidic catalyst into an activated one [29]. The pore size of 3.6 nm facilitated formation of a lower yield of C9-C15 hydrocarbons from Jatropha oil and from the algae oil than over the corresponding catalyst with the pore size of 3.8 nm (Table 4, entry 17) [31]. The former hierarchical ZSM-5 support was prepared by the hydrothermal synthesis route using a three times higher ratio of micro/mesoporous templating agents, i.e. 7.1 vs 2.4 (Table S1, entry 17). The pore size in this catalyst was varied using organosilane as a template [62]. As a mesopore directing agent, octadecyldimethyl-(3-trimethoxysilylpropyl) ammonium chloride was used and Ni was loaded via wet impregnation followed by drying and calcination of the catalyst. At the same time the HSAC catalyst, in which HSAC indicates high surface area catalyst, exhibited 2.4 fold more strong acid sites in comparison to LSAC [31] due to the presence of extra-framework Al in the former catalyst [61], which was confirmed in HSAC by ^{27}Al-MAS-NMR showing a high peak at 0° [31]. This catalyst gave a higher yield of C9-C15 hydrocarbons in Jatropha oil hydroprocessing and lower isomerization selectivity in comparison to LSAC (low surface area catalyst) (Table 2). In addition, it has been stated that for hierarchical zeolites not only the pore size, but also a higher number of acid sites in the pore mouth are important in enhancing reactivity [12].

The addition of Keggin type phosphotungstic acid to Ni-catalysts has been intensively studied [8,63,64]. For example, mesoporous MCM-41 has typically a mild acidity, which is not sufficient for an effective catalyst. One method to increase acidity of Ni-MCM-41 catalyst is to add a heteropolyacid, e.g. phosphotungstic acid ($H_3PW_{12}O_{40}$), to MCM-41 (Table 4, 18) [8,11]. This heteropolyacid exhibits the Keggin structure, in which P acts as a heteroatom, while polyatoms, such as W are bridged via oxygen in a certain pattern [63]. Addition of phosphotungstic acid to Ni catalysts was demonstrated in [8,11] (Table 4, entry 18–20). In particular 10 wt% Ni-20 wt% HPW-MCM-41 catalyst exhibited a rather large amount of strong acid sites with its pore diameter of ca. 3.5 nm being efficient in hydroconversion of methyl palmitate. Furthermore, HPW is located inside the pores of MCM-41, when the catalyst was prepared by wet impregnation (Table 4, entry 18, Table S1, entry 18) [35]. However, the specific surface area of HPW loaded Ni/MCM-41 catalyst decreased by 25% in comparison with the catalyst without HPW. With loadings higher that 20 wt% of HPW the structure partially collapsed.

In addition, phosphotungstic acid and Ni were loaded on a commercial mesoporous Y zeolite by the wetness impregnation method (Table 4, entry 19) [8]. Acidity of 10 wt% Ni/meso-Y catalysts with different HPW loadings increased with increasing the HPW content [8]. The highest amount of strong acid sites was obtained for 10 wt% Ni/meso-Y containing 4 wt% of HPW. This catalyst contained 1.8 fold more weak acid sites in comparison to strong acid sites determined by ammonia TPD and mesopores above 2 nm, although 80% of the pore volume was present in micropores [8].

When the HPW content increased above 4 wt%, it was agglomerated inside the mesopores of Y-zeolite. The specific surface area also decreased form 630 m^2/g to 480 m^2/g when increasing the HPW loading from 0 to 8 wt% [8]. The highest selectivity to the jet fuel components in microalgae biodiesel hydroconversion was obtained over 10 wt% Ni/meso-Y containing 4 wt% of HPW (Fig. 7) [8].

Co-precipitation was used to prepare 5 wt% Ni-30 wt% $H_3PW_{12}O_{40}$ supported on hydroxyapatite with high acidity and at the same time suitable interactions between Ni and W, promoting reduction of Ni (Table 4, entry 20) [11,64]. The FTIR analysis showed that the Keggin structure was preserved while XRD confirmed the hydroxyapatite structure. According to ammonia TPD acidity increased with increasing HPW loading.

Based on XPS measurements Ni was present both as Ni^0 and Ni^{2+}, while the speciation of W included W^{x+} and W^{6+}. It was additionally

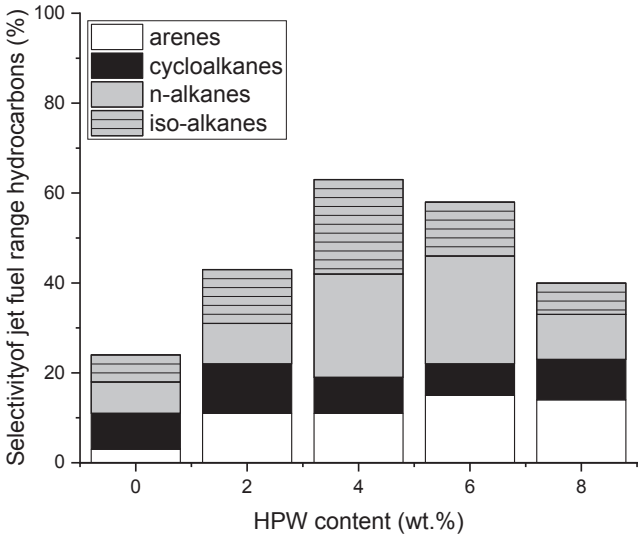

Fig. 7. Selectivity to jet fuel hydrocarbons in hydroconversion of microalgae biodiesel over 10 wt% Ni/meso Y-HPW at 255 °C under 20 bar hydrogen, adapted from [8]

stated that a high amount of acid sites can originate from interactions between Ni and HPW. 30 wt% Ni-HPW/hydroxyapatite exhibited large pores, and according to XPS the amount of Ni^0 was 2.2 fold that found in the corresponding Ni/HA catalyst in the absence of HPW [11]. It was concluded that nickel reduction was promoted due to the electron transfer between Ni and W in the presence of the Keggin type structure and at the same time more W^{6+} was found in the former catalyst than in the latter one. Catalyst acidity can be increased after addition of the Keggin type acid to the metal supported catalysts to promote the jet fuel production [11,35].

4.3. Mono- and bimetallic Co-, and Mo catalysts

Mono- and bimetallic Co, Co-Mo and Ni-Mo catalysts have been studied in hydroconversion of fatty acids [26,27,36]. Monometallic, desilicated cobalt catalyst, Co-H-MCM-49 with 5 wt% CoO, prepared by the solid state ion-exchange combined with the melt infiltration method was used in palmitic acid hydroconversion (Table 4, entry 21, Table S1, entry 26) [26]. Rather strong acid sites in Co supported on post-synthesized H-MCM-49 zeolite are required for production of isomers in palmitic acid hydroconversion [26]. This catalyst exhibited also high crystallinity (95%) compared to the parent material [26]. The support H-MCM-49 was treated with tetraethylammoium hydroxide to tailor its textural properties and acidity [65]. The desilicated H-MCM-49 exhibited 1.3 and 1.7 fold higher amounts of Brønsted and Lewis acid sites, respectively than the corresponding parent zeolite. Furthermore, the ratio between the meso- pore to micropore volume of desilicated 5 wt% CoO/MCM-49 was 2.6, while for the parent Co/MCM-49 it was 2.3 (Table, 4, entry 21) [26]. TEAOH was selected due to its lower alkalinity in comparison to NaOH in order to preserve high crystallinity of the support [65]. These properties facilitated a higher cracking activity as well as diffusion of the reactant and products. Strong acidity was present in Co-MCM-49 which was treated with tetraethylammonium hydroxide (TEAOH) (Table 4, entry 21) [26]. At the same time also morphology of the zeolite was changed and the post-synthesized zeolite exhibited more 12 member rings than 10 member rings facilitating better diffusion of the products and a higher cracking activity [26].

In some cases the oxidation state of molybdenum has been a very important parameter [36]. For monometallic 21 wt% Mo/H-ZSM-22 catalyst, calcination and reduction temperatures were optimized to increase metal reducibility (Table 4, entry 22) [36]. The Optimum calcination and reduction temperatures were determined for Mo/H-ZSM-22 catalyst, being 550 °C and 600 °C, respectively, which facilitated a partial reduction of Mo^{4+} to Mo^0 , retaining, however, the zeolite crystallinity opposite to reduction at 700 °C [36]. The catalyst calcined at 550 °C and reduced at 600 °C exhibited also a higher Mo^{4+}/Mo^{6+} ratio than after reduction at 700 °C, which was beneficial for the optimal hydrodeoxygenation to hydrodecarbonylation ratio and gave the highest I/N ratio. Furthermore, calcination at 650 °C was also too high decreasing the surface area. MoO_x species in Mo/H-ZSM-22 catalyst were uniformly located outside the channels of HZSM-22 being 20 times bigger than the channel size (Table 4, entry 22) [36].

Bimetallic sulfided 3 wt% Co-8 wt% Mo supported on mesoporous titanosilicate (MTS) catalyst exhibited a suitable pore size and 2.9 fold higher oxygen adsorption capacity, being a measure of the metal dispersion, as for the corresponding 3 wt% Co 8 wt% Mo/Al_2O_3 catalyst (Table 4, entry 23) [24]. Furthermore, its acidity was 5 fold that of $CoMo/Al_2O_3$. The support, mesoporous titanosilicate, exhibited four fold more weak than strong acid sites. A comparative work for hydroupgrading of Jatropha oil at 300 °C under 80 bar hydrogen using sulfided 3 wt% Ni- 8 wt% Mo supported on mesoporous titanosilicate (MTS) and 3 wt% Co- 8 wt% Mo /MTS, which exhibited similar acidities, showed that the former one was more active giving 85% conversion in comparison to 65% obtained for 3 wt% Co- 8 wt% Mo /MTS. In addition 3 wt% Ni 8 wt% Mo /MTS catalyst promoted formation of oligomeric products lowering thus the yield of C9-C15 products, while less oligomers were obtained over 3 wt% Co 8 wt% Mo /MTS. Unfortunately reduction of different catalysts was not investigated in [24], although it is well known that Co oxide is more difficult to be reduced than Ni oxide [44]. In addition XPS measurements would have revealed important information about the metal oxidation states.

5. Effect of reaction conditions

The effect of several reaction parameters in hydroupgrading of fatty acids and oils has been investigated including temperature, pressure, space velocity and residence time in continuous reactors at different hydrogen to feedstock ratio [1,4,8,9,22,23,31]. The main trends in conversion and selectivity are given below.

5.1. Effect of reaction temperature

The effect of the reaction temperature on hydroupgrading of fatty acids and oils has been intensively studied [2,9,12,13,17,18,20,23,25,27,32,45]. One example hydroupgrading of Jatropha oil investigated with 2 wt% Pt/SAPO-11 [17], Ni-Mo supported on hierarchical high surface area ZSM-5 [31] or $NiH_3PW_{12}O_{40}$/nanohydroxyapatite [11]. In several cases an optimum temperature was reported giving the highest yield of jet fuel components as well as the highest I/N ratio [11,17,31]. For example, in hydrotreatment of Jatropha oil over dodecyl benzene sulfonate modified 2 wt% Pt/SAPO-11 the effect of temperature on selectivity and the deoxygenation degree was studied in the range of 360–440 °C [17]. Deoxygenation degree decreased above 400 °C and at this optimum temperature the highest selectivity to the liquid products was obtained (Fig. 8) [17].

Analogously an optimum temperature of 360 °C was reported in [11] giving the highest I/N ratio in the liquid product in hydroconversion of Jatropha oil under 30 bar hydrogen over 5 wt% Ni- 30 wt% $H_3PW_{12}O_{40}$/nanohydroxyapatite. At the same time, the total liquid product yield decreased with increasing temperature due to formation of gaseous products. An optimum reaction temperature of 410 °C was also observed in algal oil hydroconversion in a trickle bed reactor operated in a narrow range of LHSV with Ni-Mo supported (5 wt% NiO, 18 wt% MoO_3) on hierarchical high surface area ZSM-5 giving maximally 54% yield of C9-C15 at 96% conversion [31].

The product distribution also changed with increasing temperature

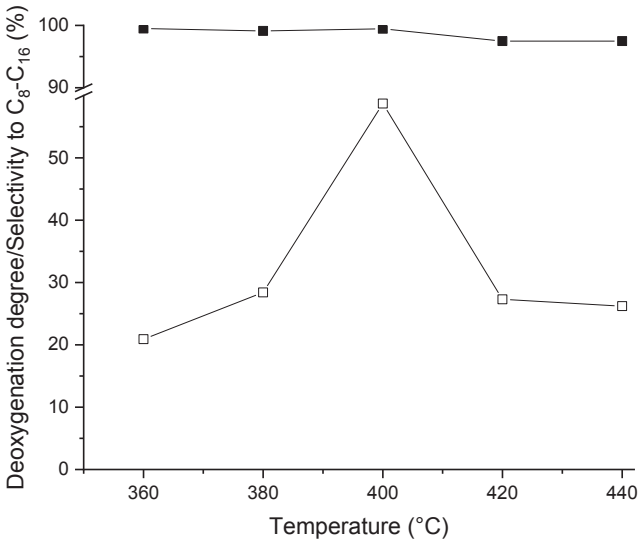

Fig. 8. Deoxygenation degree (■) and selectivity to C6-C16 hydrocarbons calculated on the mass basis among the liquid products (□) in hydroupgrading of Jatropha oil under 50 bar hydrogen using LHSV of 1.2 h^{-1} over dodecyl benzene sulfonate modified 2 wt% Pt/SAPO-11,
adapted from [17]

[22,32]. In soybean oil hydroconversion over 8 wt% Ni/SAPO-11 under 40 bar hydrogen the conversion increased from 90% at 310 °C to complete conversion at 340 °C and at the same time isomer selectivity increased with increasing temperature from 310 °C to 380 °C [32]. In addition, more cycloalkanes and aromatic compounds were formed at higher temperatures over sulfided 2.7 wt% Ni-12.7 wt% Mo/γ-Al_2O_3 under 140 bar in hydroconversion of highly unsaturated buriti oil (an Amazonian oil) [22] showing that the Diels-Alder reaction is promoted at high temperatures (Fig. 9). In the Diels-Alder reaction unsaturated fatty acids are transformed to cyclopentene (see Section 9).

The temperature effect in hydroupgrading of palm oil was studied over 10 wt% Ni/SAPO-34 in [18] and over 30 wt% NiAg/SAPO-11 [20]. In the former case the highest selectivity to the jet fuel components, 65%, was obtained with 10 wt% Ni/SAPO-34 at 390 °C–410 °C under 30 bar hydrogen, while lower temperatures resulted in lower selectivity [18]. Furthermore, NiAg/SAPO-11 gave at 380 °C only 70% selectivity to the jet fuel components (C8-C16) under 52 bar hydrogen from palm oil, while at 400 °C the corresponding selectivity was 84%. At an even higher temperature a slight decrease of selectivity to 80% was observed related to formation of the gas phase products through cracking. At the same time, the I/N ratio increased from 0.5 to 2.5 when increasing temperature form 380 to 420 °C [20].

Hydroconversion of soybean oil was performed over $NbOPO_4$ in [23,32]. The deoxygenation degree of soybean oil increased with increasing temperature from 300 °C to 350 °C under 10 bar hydrogen being 70 and 77%, respectively [23]. The product distribution changed also in hydroupgrading of soybean oil over 8 wt% Ni/SAPO-11 with increasing the reaction temperature from 310 °C to 380 °C. The main products were decarbonylated/decarbonylated products, while the isomer selectivity was 84% at 380 °C. With increasing temperature from 310 °C to 380 °C also selectivity to the cracking products, C7-C14 increased from nearly zero to 25% [32].

In hydroconversion of waste cooking oil over 25 wt% Ni- 0.5 wt% Ag/SAPO-11 selectivity to the jet fuel range alkanes decreased from 75% at 320 °C to 38% at 400 °C under 30 bar hydrogen [5]. Furthermore, catalyst deactivation was also clearly demonstrated through a decreased amount of methane in the gas phase above 380 °C. The main gaseous product was methane, which corresponded to 98% of the total peak area of the gaseous products, ethene, propane and butane.

The temperature effect in palmitic acid hydroconversion has been investigated over 5 wt% Ni and Co supported on H-ZSM-5 [27], 21.2 wt % Mo/H-ZSM-22 [25], 4 wt% Ni-H-ZSM-22 [4]. The optimum temperature for palmitic acid hydroupgrading to jet fuel components was at ca. 260 °C [4,27], much lower than for the feedstock described above. For example, palmitic acid hydroconversion over hierarchical micro- and mesoporous Ni and Co loaded with 5 wt% metal oxide H-ZSM-5 and H-HZSM-5 desilicated with tetraethylammonium hydroxyl was investigated under 40 bar hydrogen in a batch reactor using decane as a solvent [27]. The results showed that more isomers and C14 and C15 hydrocarbons were formed at 260 °C in comparison to 240 °C. A high I/N ratio and high selectivity to iso-C16 were obtained over Co supported on mesoporous H-ZSM-5 at 260 °C under 40 bar hydrogen. Analogously the fraction of isoalkanes increased in hydroconversion of palmitic acid when increasing temperature from 240 to 260 °C over desilicated Ni/HZM-5 catalyst (5 wt% NiO) giving more cracking products [27]. 21.2 wt% Mo/ZSM-22 catalyst promoted formation of the jet fuel components from palmitic acid at 260 °C giving also a high I/N ratio [25]. Analogously the I/N ratio increased in palmitic acid hydroconversion over 4 wt% Ni-H-ZSM-22 in the temperature range of 150 – 260 °C under 40 bar in 4 h [4].

The temperature effect was investigated in oleic acid hydroconversion over tetraoxysilane treated 10 wt% Ni/ZSM-5 nanosheets [12] and 4 wt% Ni/Al_2O_3 prepared by the atomic layer epitaxy (ALE) method [13]. An optimum temperature of 250 °C under 30 bar hydrogen gave the highest yield of the aviation fuel range alkanes (AFRA, C9-C15), ca. 52% with the I/N ratio of 1.7. The organic liquid product yield was slightly higher at 250 °C than either at 240 °C or 260 °C, being ca. 78% at 250 °C. Furthermore, it was observed that the I/N ratio increased with increasing temperature from 240 °C to 260 °C [12]. On the other hand, Ni/Al_2O_3 (ALE) catalyst with a high metal dispersion exhibited an optimum activity under 30 bar hydrogen for hydroconversion oleic acid at 360 °C giving ca. 37% selectivity to AFRA, while at a higher temperature this catalyst was too active for hydroconversion giving ca. 80% selectivity to C4-C8 hydrocarbons [13].

5.1.1. *Effect of pressure*

The effect of pressure has been investigated in several studies [5,9,12,17,20], typically showing existence of an optimum pressure promoting formation of the jet fuel components [5,20]. For example, an optimum pressure was obtained in hydroconversion of palm oil at 400 °C in the pressure range of 38–59 bar over 30 wt% NiAg/SAPO-11 (Fig. 10) [20]. This was explained by enhanced cracking at a high temperature and pressure and at the same time, reaction of hydrogen with free radicals formed in the cracking reactions suppresses

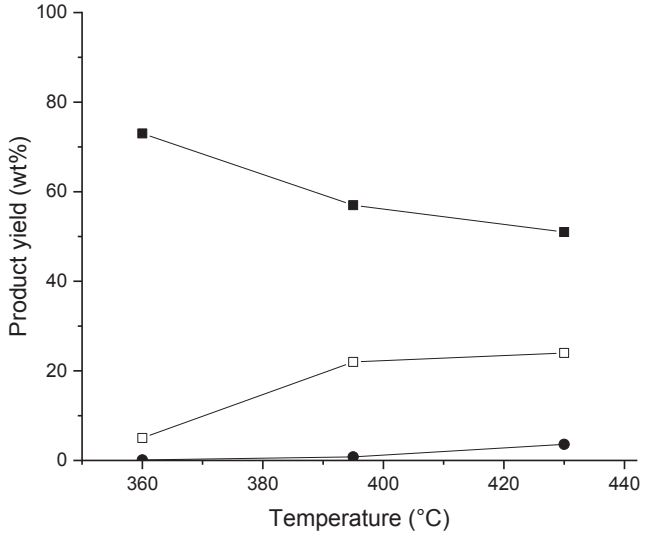

Fig. 9. Effect of temperature on formation of alkanes (■), cycloalkanes (□) and alkylbenzene (●) in hydroconversion of buriti oil at 140 bar for 2 h over sulfided 2.7 wt% Ni-12.7 wt% Mo/γ -Al_2O_3,
adapted from [22]

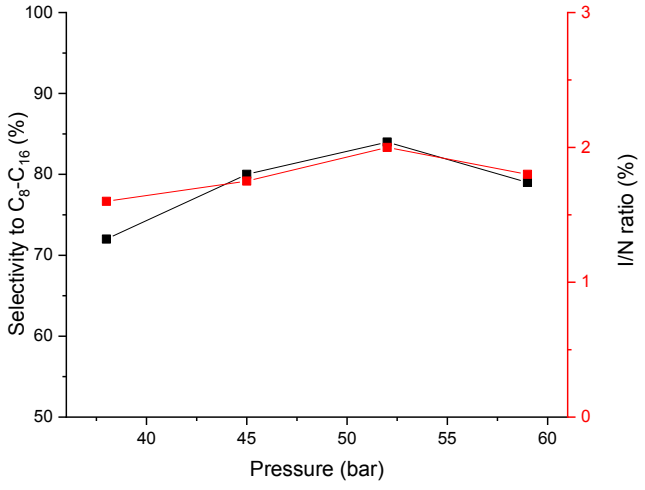

Fig. 10. Selectivity to C8-C16 hydrocarbons (■) and I/N ratio (●) in hydroconversion of palm oil over mesoporous 30 wt% NiAg-SAPO- 11,
adapted from [20]

isomerization [66].

A high hydrogen pressure increased slightly the yield of C9-C14, while the diesel yield was influenced more, increasing from 18% to 66% when the pressure was increased from 20 to 90 bar in hydroconversion of Jatropha oil over Ni/W/SiO_2-Al_2O_3 catalyst at 420 °C (Fig. 11) [2]. It was concluded in [2] that the pressures above 60 bar promote the C-O cleavage while the C–C cleavage is preferred below 60 bar over 4 wt% Ni- 24 wt% W/SiO_2-Al_2O.

On the other hand, above 40 bar in Jatropha oil hydroconversion over sulfided CoMo/Al_2O_3 catalyst at 360 °C the most prominent products were C15-C18 compounds, while the yield of C9-C14 hydrocarbons decreased from 12% to 7% with increasing pressure from 20 to 90 bar [1]. Analogously to [1] the highest I/N ratio, 1.5 was obtained in hydroconversion of Jatropha oil at 400 °C over sodium dodecylbenzene sulfonate (SDBS) modified 2 wt% Pt/SAPO-11 under 40 bar. Above that pressure hydrogenation of the hydrolyzed oil and the subsequent dehydrogenation step, which is catalyzed by the metal, are retarded inhibiting also the following steps, such as isomerization. Pressure changes in hydroconversion of Jatropha oil at 400 °C over dodecylbenzene sulfonate modified SDBS-2 wt% Pt/SAPO-11 did not show any clear influence on C8-C16 selectivity [17].

In hydroconversion of waste cooking oil, it was pointed out that over 25 wt% Ni- 0.5 wt% Ag/SAPO-11 the hydrogen pressure of 20 bar was sufficient to maintain the balance between hydrogenation and dehydrogenation, keeping the methane formation at a low level. On the other hand, at higher hydrogen pressures methane formation increased due to higher cracking [5].

Buriti oil hydroconversion was performed over sulfided 2.7 wt% Ni-12.7 wt% Mo/γ-Al_2O_3 catalyst under high pressure giving alkanes [22], while formation of cycloalkanes and alkylbenzene was not affected by the increased pressure.

In oleic acid hydroconversion oleic acid at 250 °C conversion increased from 50 to ca. 100% when increasing the hydrogen pressure from 4 to 30 bar [12]. At the same time, the organic liquid product yield increased from 30% to 78%. However, only a minor pressure effect on the I/N ratio, increasing it 1.6 fold, was observed over 10 wt% Ni/ZSM-5 nanosheet catalyst at 250 °C in the pressure range of 4 to 30 bar [12]. A similar result was reported for Jatropha oil hydroconversion over the surfactant modified 2 wt% Pt/SAPO-11 [17]. At the same time, lower hydroisomerization activity is observed at a lower hydrogen pressure.

5.1.2. Effect of H_2/feedstock ratio

The effect of hydrogen to feedstock ratio has been investigated in hydroconversion of waste cooking oil [5], Jatropha oil [17] and palm oil [20]. An optimum H_2/feedstock molar ratio of 12.8 was found in the former case with 25 wt% Ni-0.5 wt% Ag/SAPO-11 at 380 °C under 40 bar hydrogen at WHSV of 2 h^{-1} [5]. Analogously a maximum H_2/feedstock ratio was determined in hydroconversion of Jatropha oil over SDBS-Pt/SAPO-11 giving the highest yield of C_8-C_{16} [17]. Conversion of Jatropha oil increased with increasing the H_2/feed ratio over Co-Mo/Al_2O_3 [1], lowering at the same time the yield of oligomers, while the yield of heavy C_{15}-C_{18} hydrocarbons increased and the fractional yield of C_9-C_{14} was only mildly affected.

5.1.3. Effect of conversion

The effect of conversion was investigated by changing the space velocity and the residence time in hydroconversion of fatty acids and oils [1–3,9,15,17,20]. Typically, as can be anticipated, higher amounts of jet fuel components were obtained with low space velocities [1,5,9]. Examples include Jatropha oil hydroconversion 3.3 wt% CoO-12 wt% MoO_3/Al_2O_3 [67] and Ni-W-SiO_2-Al_2O_3 catalysts [1,2] as well as hydroconversion of waste cooking oil over 25 wt% Ni- 0.5 wt% Ag/SAPO-11 [5]. Conversion of Jatropha oil decreased also with increasing space velocity over sulfided 4 wt% NiO-24 wt% WO_3/SiO_2-Al_2O_3 at 420 °C under 80 bar hydrogen when using H_2/feed ratio of 1500 vol/vol [3]. The highest fractional yield of C9-C14 hydrocarbons, 72%, in Jatropha oil hydroconversion was obtained over 4 wt% NiO-24 wt% WO_3/SiO_2-Al_2O_3 catalyst in a fixed bed reactor at 420 °C under 80 bar hydrogen with 0.5 h^{-1} space velocity, while it decreased rapidly with increasing space velocity (Fig. 12) [3]. At the same time, the yield fraction of C_9-C_{14} hydrocarbons decreased from 12% to 4% and the yield of heavy compounds increased [1]. However, under these conditions, a hot spot corresponding to the temperature of 737 °C was observed in the upper part of the catalyst bed and ca. 340 °C temperature gradient across the bed was observed due to high exothermicity of the reaction [3]. This result clearly showed a need of the liquid/gas quench streams to avoid temperature run-away.

On the other hand, Ni/HZ-1 was more active than Co-HZSM-5 with 5 wt% CoO in [27] in hydroconversion of palmitic acid, because C15 is the main product after 0.5 h in the reaction mixture. This is the third product in the consecutive route, i.e. first hexadecane is formed from palmitic acid, followed by isomerization to methylpentadecane, which is further cracked to pentadecane. In addition, when the space velocity is increased from 1 h^{-1} to 8 h^{-1} in Jatropha oil hydroconversion at 360 °C

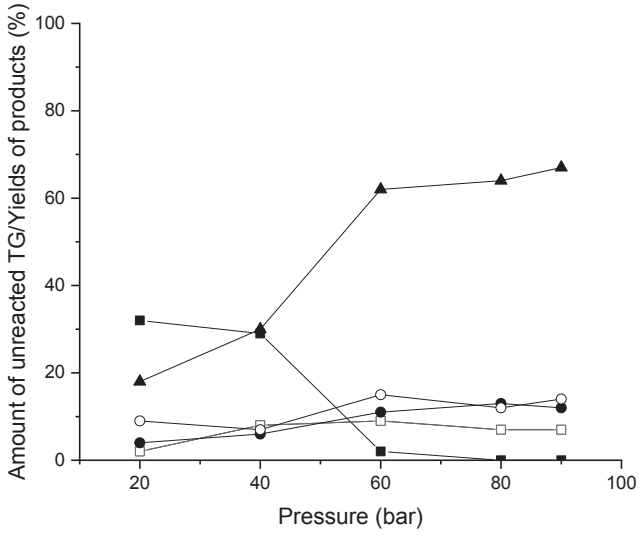

Fig. 11. Effect of pressure in hydroconversion of Jatropha oil at 420 °C in a continuous reactor over sulfided 5 wt% NiO-18 wt% MoO_3/H-ZSM-5 catalyst adapted from [2]. Notation: (■) unconverted triglycerides, (□) < C9, (●) C9-C14, (▲) C15-C18, (o) > C18.

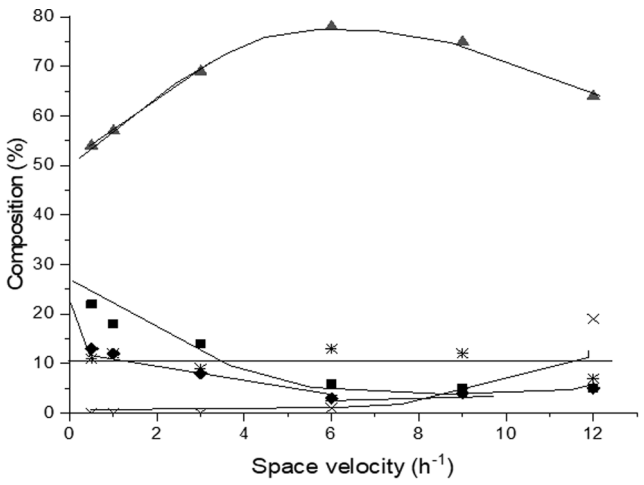

Fig. 12. The product yields in hydroconversion of Jatropha oil over sulfided 4 wt% NiO-24 wt% WO_3/SiO_2-Al_2O_3 at 420 °C under 80 bar hydrogen as a function of space velocity. Symbols: (◆) < C9, (■) C9-C14, (▲) C15-C18, (*) > C18 adapted from [3]. The lines represent modelling results.

under 80 bar over sulfided $CoMo/Al_2O_3$ complete conversion of oil was obtained [1].

At low space velocities more isomers were formed in soybean oil hydroconversion at 370 °C under 40 bar hydrogen using 300 ml/min flow of hydrogen over 8 wt% Ni/SAPO-11 [32]. It was also demonstrated in [15] that longer residence times gave more aromatic products in hydroconversion of soybean oil over 1 wt% Pt/Al_2O_3/SAPO-11 at 370 °C under 30 bar hydrogen [15]. Furthermore, concentration profiles as a function of residence time indicate parallel hydrogenation and aromatization.

In hydroconversion of refined bleached deodorized palm oil the optimized reaction conditions for production of jet fuel components were 477 °C, 56 bar and 1.5 h over a non acidic Pd/Al_2O_3 catalyst and it was concluded that higher jet fuel yields were obtained with increasing both temperature and LHSV [9].

6. Catalyst stability and long-term performance

Catalyst regeneration and recycling has been intensively studied [8,11,13,16,26,27,31]. In some cases, very stable conversion and selectivity towards different products were obtained, for example in hydroconversion of microalgae based biodiesel over 10 wt%/Ni-4 wt% HPW/meso Y [8], hydroconversion of Jatropha oil over 5 wt% Ni-30 wt % HPW on hydroxyapatite [11], in the two step process to produce jet fuels form palm oil over Pt/γ-Al_2O_3 and in the second step transforming long chain hydrocarbons over Pt/Nano-Beta zeolite [16]. On the other hand, changes in the product distribution in catalyst recycling was observed in hydroconversion of palmitic acid over 21 wt% Mo/ZSM-22 [25], over 4 wt% Ni-H-ZSM-5 [4] and in oleic acid hydroconversion over 4 wt% Ni/Al_2O_3 prepared by ALD [13]. It should, however, be pointed out that in hydroconversion of palmitic acid over desilicated Co/HMCM-49 (5 wt% CoO) only minor changes in the product distribution were observed and conversion, of 99.9% remained the same [26]. This result is important showing suitability of the desilicated bifunctional Co-MCM-49 with large pores and strong acid centers to be used as a catalyst for palmitic acid hydroconversion.

The performance of 5 wt% Ni-30 wt% HPW on hydroxyapatite was very stable in Jatropha oil hydroconversion at 360 °C under 30 bar hydrogen for 196 h time-on-stream [11]. Thermogravimetric analysis of the spent catalyst showed that only 4.3 wt% carbon was accumulated on the catalyst surface. Furthermore, 10 wt% Ni- 4 wt% HPW/meso Y exhibited very stable performance in transformations of microalgae based biodiesel giving 61% selectivity of jet biofuel with 97% conversion during 24 h time-on-stream [8]. Sulfided Ni-Mo/ZSM-5 with a high specific surface area (HSAC) containing 5 wt% of NiO and 18 wt% of MoO_3, could be reused in algal oil hydroconversion after regeneration at 450 °C with an air stream and resulfidation [31]. In [31], however, no further details were provided about recycling. When recycling 25 wt% Ni- 0.5 wt% Ag/SAPO-11 catalyst in hydroconversion of waste cooking oil [5], some changes in the catalyst properties occurred, such as a change of the Ni particle shape as well as disappearance of acid sites.

A very stable performance of 1 wt% Pt/Al_2O_3 was observed for transforming palm oil to long chain fatty acids under 20 bar hydrogen at 360 °C for 4 days followed by hydroconversion of the obtained product with 1 wt% Pt/nano-Beta zeolite at 235 °C under 20 bar hydrogen [16]. Namely, the C8-C16 yield was 72% after 24 h (71%) after 4 days with the corresponding to I/N ratios of 7.5 and 7.8 [16]. As a comparison the one-step process for palm oil hydroconversion was also investigated over 1 wt% Pt-Nano-Beta at 295 °C under 20 bar hydrogen using WHSV of 2 h^{-1}. The product distribution in that case changed from 2 h time-on-stream with the main product in the hydrocarbon range of 4–8 to mainly C15-C18 at 24 time-on-stream.

Morphology changes of Ni particles were observed in NiAg-SAPO-11 catalyst after its utilization in waste cooking oil hydroconversion [12]. Polyhedral Ni particles found in the fresh catalyst were transformed to the spherical ones after the reaction, when the catalyst was used in hydroconversion of waste cooking oil. XRD patterns from the fresh and spent NiAg/SAPO-11 catalysts were, however, nearly identical showing the metal particle size did not vary. On the other hand, the Ni particle size according to TEM measurements in 10 wt% Ni/ZSM-5 nanosheets was ca. 10 nm and only slight sintering occurred in hydroconversion of oleic acid at 250 °C under 30 bar hydrogen [12]. Furthermore, the MFI structure of the zeolite support remained intact.

7. Reaction kinetics in the batch mode

Hydroconversion of fatty acids and oils has been typically investigated in continuous reactors [1–3,8,10–12,15–17,20,21,24,29,31–33], while batch reactor studies have been scarcely made [18,22,25,28,38]. Among these studies only a few have reported kinetic data as a function of time [4,26,27].

Reaction kinetics in hydroconversion of palmitic acid has been intensively studied [4,27]. The concentrations of different products as a function of reaction time in palmitic acid hydroconversion reveal that deoxygenation is not completed after 30 min because a small amount of hexanoic aldehyde is present in the reaction mixture and conversion of palmitic acid at this point is ca. 95% [27]. The main product is hexadecane with its yield passing through a maximum at 1 h after which methylpentadecane is formed (iso-C16). After prolonged times also small amounts of methyltetradecane as well as lighter cracking products, C13 and C14 are formed (Fig. 13).

The normalized selectivity of different products with carbon numbers ranging from C12 to C16 as a function of time was reported in palmitic acid hydroconversion under similar conditions as above over Co/HMP-49 in [26]. Both selectivity to C16 and C15 passed through a maximum forming C12- C14 hydrocarbons indicating that this catalyst was also very active in hydroconversion in comparison to 4 wt% Ni/HZM-22 (Fig. 14) [4] and Co-H-ZSM-5 (5 wt% CoO) [27].

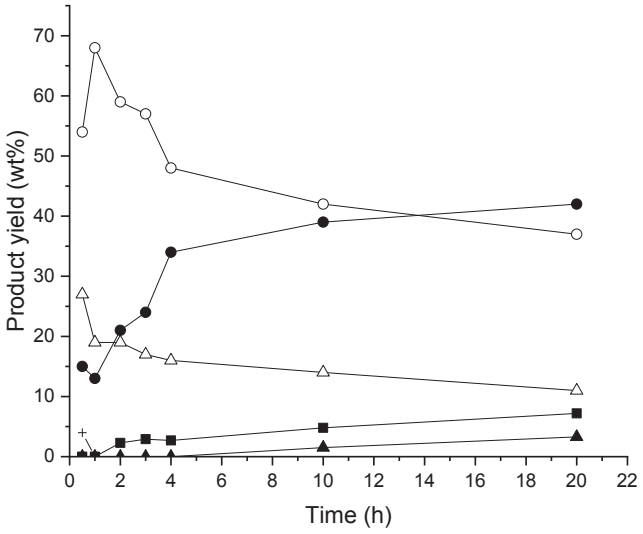

Fig. 13. The fractional product yield as a function of reaction time in hydroconversion of palmitic acid in decane as a solvent at 260 °C under 40 bar hydrogen over post-treated Co/H-ZSM-5 (5 wt% CoO), adapted from [27]. Notation: hexadecanal C15-CHO (+), n-C16 (o), iso-C16 (●), n-C15 (Δ), iso-n C15 (▲) and cracking products (■).

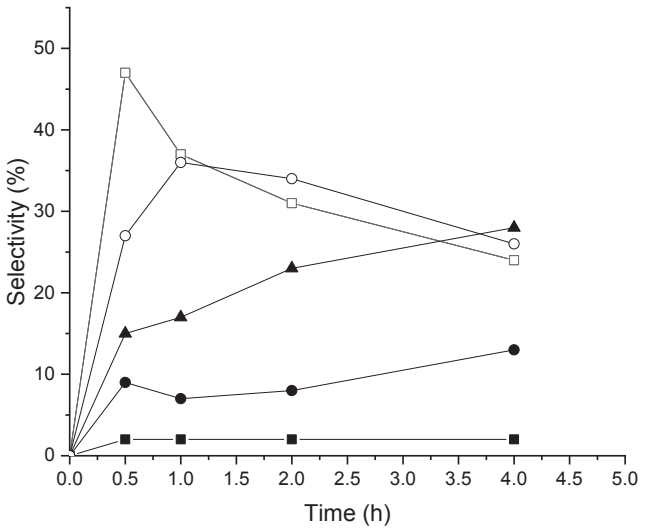

Fig. 14. Selectivity to n-C14 (■), n-C15 (□), iso-C15 (●), n-C16 (o), iso-C16 (▲) in hydroconversion of palmitic acid over 4 wt% Ni-/H-ZSM-22 at 260 °C under 40 bar in a batch reactor,
adapted from [4]

8. Kinetic modelling of hydroconversion of oils and fatty acids

Several kinetics models were tested for hydroconversion of Jatropha in a fixed bed reactor over mesoporous sulfided 4 wt% NiO-24 wt% WO_3/SiO_2-Al_2O_3 [3] and for $CoMo/Al_2O_3$ hydrotreating catalyst, when both temperature and pressure were changed. Furthermore, the H_2/feed ratio and space time were also varied [1,24]. For the former catalyst, which also exhibited acidic properties, more kerosene products were formed, especially at high temperature. Formation of C9-C14 components was the most prominent at 420 °C under 80 bar hydrogen with a low space velocity. The most suitable model contains both parallel formation of oligomers, heavy, middle and naphtha components and a consecutive route from heavy to kerosene and further to naphtha compounds. The model involves several different lumped kinetic constants.

Both diffusivity of different compounds at a given temperature as well as the effectiveness factor, i.e. the ratio between the rate in the presence of mass transfer limitations and the rate in the kinetic regime, were calculated in [3]. The results showed that the effectiveness factor was close to one and the experiments were performed in the diffusion free region. In addition, activation energies were determined for formation of different product groups. The activation energy for transformation of triglycerides is 115 kJ/mol, which it was nearly the same as for formation of diesel, 122 kJ/mol, while higher activation energies were required for formation of naphtha and kerosene, being 130 kJ/mol and 122 kJ/mol, respectively. These results clearly show that a high energy input is required for formation of kerosene and naphtha type compounds. Furthermore, temperature profile along the catalyst bed was calculated. Considering heat of reactions determined separately for different reactions, i.e. depropanation, hydrodeoxygenation, decarboxylation, decarbonylation and hydrocracking. The results showed that exothermicity of hydroconversion of Jatropha oil was very high, 1.34 MJ/kg Jatropha oil, which is nearly 10 fold of the heat released in cracking of vacuum gas oil [68].

It was also observed for hydroconversion of Jatropha oil that for 3 wt % Co-8 wt% Mo/Al_2O_3 the above mentioned model was valid at 360 °C, while another type of parallel-consecutive route was describing better the results below 320 °C [29].

Due to a higher acidity of 3 wt% Co-8 wt% Mo/MTS in comparison to 3 wt% Co-8 wt% Mo/Al_2O_3, the best fitting model for Jatropha oil hydroconversion was based on the parallel direct formation of different fractions at 300 °C [29].

9. Reaction mechanism

The reaction mechanism in hydroconversion of oils [3,16,17,22,23,29,32], fatty acids [4,12,26,25,27,28,45] and their esters [37] has been intensively studied. Hydroconversion of oils starts with hydrogenation of triglycerides (TG) to the corresponding saturated molecules [29], followed by depropanation [15,20]:

$$TG + H_2 \rightarrow R_xCOOH + CH_3CH_2CH_3 \quad (2)$$

Thereafter, fatty acids undergo either hydrodeoxygenation forming water and a hydrocarbon with the same amount of carbon as in the original fatty acid, or alternatively undergoes decarbonylation or decarboxylation forming a hydrocarbon with one carbon less and CO or CO_2, respectively [29]. It was also proposed in [15] that fatty acids formed via hydrolysis of triglycerides can be dehydrogenated forming triene fatty acids, which are transformed to conjugated double bonds [15]. Five-membered hydrocarbon rings are formed by the intermolecular Diels-Alder reaction of the conjugated triene over Lewis acid sites [69]. For example, dodecylbenzene, a product in hydrocracking of soybean oil is formed by a migration of double bonds from C9 to C15 in linoleic and linolenic acids to the terminal position of the hydrocarbon chain before the intermolecular Diels-Alder reaction takes place [15]. It was also reported in [20] that cyclic hydrocarbons are converted to aromatics by ring expansion over Ni and Lewis acid sites. In hydrogenolysis of oils, propane and C6-C8 olefins are formed. Propane can be dehydrogenated to propene and react with C6-C8 olefins. Aromatic compounds can also be formed from e.g. butadiene and ethane, giving first cyclohexene by the Diels-Alder reaction followed by dehydrogenation of cyclohexene [23]. Furthermore, substituted cyclopentane derivatives undergo easily a ring expansion forming for example 1-methylcyclohex-1-ene and toluene [45].

In conjugated trienes the double bond migration towards the end of the carbon chain is followed by hydrodeoxygenation of fatty acids. Diesel range hydrocarbons should be dehydrogenated, isomerized and cracked to form kerosene and gasoline [29], while formation of gaseous products should be avoided. In addition to these products, also oligomers can originate from alkylation reactions [29].

The reaction mechanism in triolein hydroconversion was proposed based on the product distribution. Hexadecane is formed by γ-hydrogen transfer (Fig. 15) [23,70], while oleic acid is generated by β-elimination. Pentadecane formation requires $\beta-\gamma$ scission [23].

Different types of β-scission mechanisms for alkylcarbenium ions, proposed in the literature, are shown in Fig. 16 [16]. It has been proposed that mono-, di- and multibranched alkanes are formed in a consecutive manner.

Cracking of tribranched A type (Fig. 16) alkanes produces two branched molecules, while cracking of a dibranched B molecule gives one linear and one branched product. Furthermore, cracking of monobranched compound C generates only linear products. The relative rates for β-scission as reported in [71] decrease with a decreasing number of branching as follows: $r_A > r_{B1} \approx r_{B2} > r_C \gg r_D$.

The reaction scheme for hydroconversion of palmitic acid was proposed in [29] including palmitic acid hydrogenation to hexadecanal and further to hexadecanol, its dehydration forming hexadecane and further isomerization products by dehydrogenation, and cracking products, e.g. C13 and C13 isomer. In addition, a parallel route was proposed to hydrogenation of palmitic acid, i.e. direct hydroconversion from palmitic acid to C14. Hexadecanal can also decarbonylate and further crack and isomerize forming C12 hydrocarbons.

10. Future research needs and conclusions

Although research on production of jet fuels from fatty acids and oils has been very intensive during recent years, several future research needs could be still identified. Typically, a comprehensive product

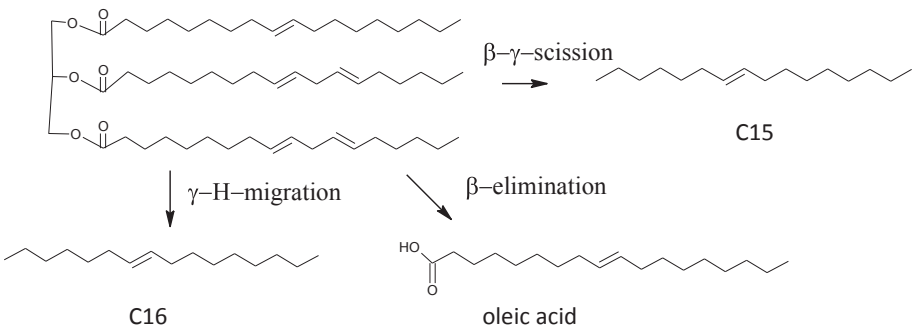

Fig. 15. Hydrotransformations of triglycerides, adapted from [23]

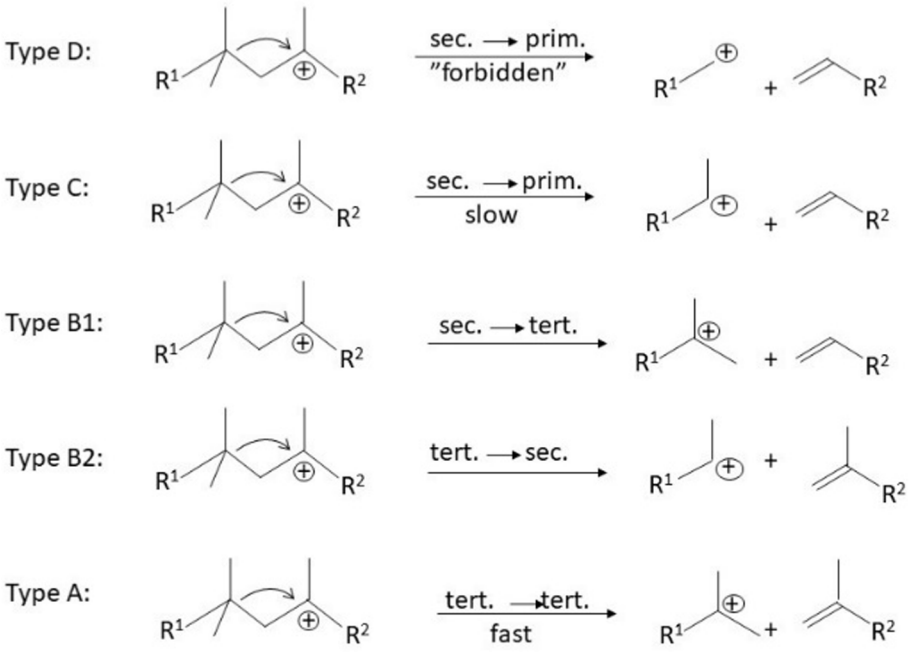

Fig. 16. Proposed β-scission mechanisms for alkylcarbenium ions, adapted from [16]

analysis with a proper mass balance closure, kinetic modelling and thermodynamic analysis have been very scarcely performed [3]. Information of fractional selectivity among liquid phase products is certainly not sufficient for eventual industrial implementation. Thus, future research efforts should be clearly focused on development of suitable analytical approaches for identification as well as quantification of products. Moreover, the broad product distribution adhering to both diesel and jet fuel fraction implies that separation of these products by distillation would be required. In addition if the concentration of aromatics is too high after hydroconversion they should be removed most probably by extraction as typically done in oil refining.

Furthermore, due to harsh reaction conditions, for example in hydroconversion of vegetable oils over Ni–W/SiO_2-Al_2O_3 many carbonaceous species are present in the gas phase (ca. 30 wt%). On the other hand, a two-step process for hydroconversion of palm oil involving hydroisomerisation over Pt/Al_2O_3 in the first step followed by hydrocracking with Pt/Beta zeolite was shown to be more feasible and not suffering extensive catalyst deactivation opposite to the one-step process.

The importance of diffusional limitations for formation of C8-C16 was clearly demonstrated showing a beneficial use of nanosized zeolites as supports. Catalyst acidity is an important parameter and although it has been measured in several publications, many papers report only qualitative data on acidity, making comparison of the results in different publications challenging.

Finally comprehensive catalyst characterization, such as determination of acidity, metal particle size, reducibility and metal oxidation states, especially using hydrogen temperature programmed reduction [2,3,11,30,32] and XPS [2,3,30,32] would bring more knowledge helping to rationalize the catalyst selection, which at the moment is largely missing [24].

In summary, production of jet fuels by hydroconversion of vegetable oils and fatty acids has been intensively studied during the recent years. The highest yields of organic liquid products, above 80 wt%, have been obtained from Jatropha and palm oil using Ni supported on $H_3PW_{12}O_{40}$/nanosized hydroxyapatite in one step at 360 °C under 30 bar hydrogen [11] and in a two-step process over Pt/Al_2O_3 (hydroisomerization at 395 °C) followed by hydrocracking at 245 °C over Pt on H-Y zeolite [15]. Jet fuel yields are typically maximally ca. 54%, while also other products such as diesel, are formed.

Declaration of Competing Interest

The authors declare that they have no known competing financial interests or personal relationships that could have appeared to influence

the work reported in this paper.

Appendix A. Supplementary data

Supplementary data to this article can be found online at https://doi.org/10.1016/j.fuel.2021.121673.

References

[1] Anand M, Sinha AK. Temperature-dependent reaction pathways for the anomalous hydroconversion of triglycerides in the presence of sulfided Co–Mo-catalyst. Bioresour Technol 2012;126:148–55.
[2] Anand M, Farooqui SA, Kumar R, Joshi R, Kumar R, Sibi MG, et al. Optimizing renewable oil hydroconversion conditions for aviation bio-kerosene production. Fuel Proc Technol 2016;151:50–8.
[3] Anand M, Farooqui SA, Kumar R, Joshi R, Kumar R, Sibi MG, et al. Kinetics, thermodynamics and mechanisms for hydroprocessing of renewable oils. Appl Catal A Gen 2016;516:144–52.
[4] Cao Y, Shi Y, Bi Y, Wu K, Hu S, Wu Y, et al. Hydrodeoxygenation and hydroisomerization of palmitic acid over bi-functional Co/H-ZSM-22 catalysts. Fuel Proc Technol 2018;172:29–35.
[5] Chen Y-K, Hsieh C-H, Wang W-C. The production of renewable aviation fuel from waste cooking oil. Part II: Catalytic hydro-cracking/isomerization of hydro-processed alkanes into jet fuel range products. Renew Energy 2020;157:731–40.
[6] Chen L, Li H, Fu J, Miao C, Lv P, Yuan Z. Catalytic hydroprocessing of fatty acid methyl esters to renewable alkane fuels over Ni/HZSM-5 catalyst. Catal Today 2016;259:266–76.
[7] Cheng J, Li T, Huang R, Zhou J, Cen K. Optimizing catalysis conditions to decrease aromatic hydrocarbons and increase alkanes for improving jet biofuel quality. Bioresour Technol 2014;158:378–82.
[8] Cheng J, Zhang Z, Zhang X, Liu J, Zhou J, Cen K. Hydrodeoxygenation and hydroconversion of microalgae biodiesel to produce jet biofuel over $H_3PW_{12}O_{40}$-Ni/hierarchical mesoporous zeolite Y catalyst. Fuel 2019;245:384–91.
[9] Dujjanutat P, Kaewkannetra P. Production of bio-hydrogenated kerosene by catalytic hydroconversion from refined bleached deodorised palm/palm kernel oils. Renew Energy 2020;147:464–72.
[10] Eller Z, Varga Z, Hancsók J. Advanced production process of jet fuel components from technical grade coconut oil with special hydroconversion. Fuel 2016;182:713–20.
[11] Fan K, Liu J, Yang X, Rong L. Hydroconversion of Jatropha oil over Ni-$H_3PW_{12}O_{40}$/nano-hydroxyapatite catalyst. Int J Hydrogen Energy 2014;39(8):3690–7.
[12] Feng F, Niu X, Wang Li, Zhang X, Wang Q. TEOS-modified Ni/ZSM-5 nanosheet catalysts for hydroconversion of oleic acid to high-performance aviation fuel: effect of acid spatial distribution. Micropor Mesop Mater 2020;291:109705. https://doi.org/10.1016/j.micromeso.2019.109705.
[13] Feng F, Shang Z, Wang Li, Zhang X, Liang X, Wang Q. Structure-sensitive hydroconversion of oleic acid to aviation-fuel-range-alkanes over alumina-supported nickel catalyst. Catal Commun 2020;134:105842. https://doi.org/10.1016/j.catcom.2019.105842.
[14] Ishihara A, Fukui N, Nasu H, Hashimoto T. Hydroconversion of soybean oil using zeolite–alumina composite supported NiMo catalysts. Fuel 2014;134:611–7.
[15] Jeong H, Bathula HB, Kim TW, Han GB, Jang JH, Jeong B, et al. Superior long-Term Stability of a mesoporous alumina-supported Pt catalyst in the hydrodeoxygenation of palm oil. ACS Sustain Chem Eng 2021;9(3):1193–202.
[16] Kim MY, Kim JK, Lee ME, Lee S, Choi M. Maximizing biojet fuel production from triglyceride: importance of the hydroconversion catalyst and separate deoxygenation/hydroconversion steps. ACS Catal 2017;7(9):6256–7.
[17] Li X, Chen Y, Hao Y, Zhang Xu, Du J, Zhang A. Optimization of aviation kerosene from one-step hydrotreatment of catalytic Jatropha oil over SDBS-Pt/SAPO-11 by response surface methodology. Renew Energy 2019;139:551–9.
[18] Li T, Cheng J, Huang R, Yang W, Zhou J, Cen K. Hydroconversion of palm oil to jet biofuel over different zeolites. Int J Hydrogen Energy 2016;41(47):21883–7.
[19] Li T, Cheng J, Huang R, Zhou J, Cen K. Conversion of waste cooking oil to jet biofuel with nickel-based mesoporous zeolite Y catalyst. Bioresour Technol 2015;197:289–94.
[20] Lin C-H, Wang W-C. Direct conversion of glyceride-based oil into renewable jet fuels. Renew Sustain Energy Rev 2020;132:110109. https://doi.org/10.1016/j.rser.2020.110109.
[21] Rabaev M, Landau MV, Vidruk-Nehemya R, Koukouliev V, Zarchin R, Herskowitz M. Conversion of vegetable oils on Pt/Al_2O_3/SAPO-11 to diesel and jet fuels containing aromatics. Fuel 2015;161:287–94.
[22] da Rocha Filho GN, Brodzki D, Djéga-Mariadassou G. Formation of alkanes, alkylcycloalkanes and alkylbenzenes during the catalytic hydroconversion of vegetable oils. Fuel 1993;72(4):543–9.
[23] Scaldaferri CA, Pasa VMD. Production of jet fuel and green diesel range biohydrocarbons by hydroprocessing of soybean oil over niobium phosphate catalyst. Fuel 2019;245:458–66.
[24] Sharma RK, Anand M, Rana BS, Kumar R, Farooqui SA, Sibi MG, et al. Jatropha-oil conversion to liquid hydrocarbon fuels using mesoporous titanosilicate supported sulfide catalysts. Catal Today 2012;198(1):314–20.
[25] Shi Y, Cao Y, Duan Y, Chen H, Chen Yu, Yang M, et al. Upgrading of palmitic acid to iso-alkanes over bi-functional Mo/ZSM-22 catalysts. Greem Chem 2016;18(17):4633–48.
[26] Shi Y, Li R, Shen Q, Yang M, Wu Y. The selective production of jet fuel range alkanes via the catalytic upgrading of palmitic acid over Co/HMCM-49 catalysts. Chem Commun 2019;55(80):12096–9.
[27] Shi Y, Xing E, Cao Y, Liu M, Wu K, Yang M, et al. Tailoring product distribution during upgrading of palmitic acid over bi-functional metal/zeolite catalysts. Chem Eng Sci 2017;166:262–73.
[28] Shi Y, Zhang J, Xing E, Xie Y, Cao H. Selective production of jet-fuel-range alkanes from palmitic acid over Ni/H-MCM-49 with two independent pore systems. Ind Eng Chem Res 2019;58(47):21341–9.
[29] Sinha AK, Anand M, Rana BS, Kumar R, Farooqui SA, Sibi MG, et al. Development of hydroprocessing route to transportation fuels from non-edible plant-oils. Catal Surveys Asia 2013;17(1):1–13.
[30] Srihanun N, Dujjanutat P, Muanruksa P, Kaewkannetra P. Biofuels of green diesel–kerosene–gasoline production from palm oil: effect of palladium cooperated with second metal on hydroconversion reaction. Catalysts 2020;10(2):241.
[31] Verma D, Kumar R, Rana BS, Sinha AK. Aviation fuel production from lipids by a single-step route using hierarchical mesoporous zeolites. Energy Environ Sci 2011;4(5):1667–71.
[32] Wang C, Liu Q, Song J, Li W, Li P, Xu R, et al. High quality diesel-range alkanes production via a single-step hydrotreatment of vegetable oil over Ni/zeolite catalyst. Catal Today 2014;234:153–60.
[33] Zhang Z, Wang Q, Chen H, Zhang X. Hydroconversion of waste cooking oil into green biofuel over hierarchical USY-supported NiMo catalyst: a comparative study of desilication and dealumination. Catalysts 2017;7(10):281. https://doi.org/10.3390/catal7100281.
[34] Zhang Z, Wang Q, Chen H, Zhang X. Hydroconversion of waste cooking oil into bio-jet fuel over a hierarchical NiMo/USY@ Al-SBA-15 zeolite. Chem Eng Technol 2018;41(3):590–7.
[35] Zhang Z, Cheng J, Zhu Y, Guo H, Yang W. Jet fuel range hydrocarbons production through competitive pathways of hydroconversion and isomerization over HPW-Ni/MCM-41 catalyst. Fuel 2020;269:117465.
[36] Zhang J, Shi Y, Cao H, Wu Y, Yang M. Conversion of palmitic acid to jet fuel components over Mo/H-ZSM-22 bi-functional catalysts with high carbon reservation. Appl Catal A Gen 2020;608:117847. https://doi.org/10.1016/j.apcata.2020.117847.
[37] Zhang Ze, Cheng J, Qiu Yi, Zhang Xi, Zhou J, Cen K. Competitive conversion pathways of methyl palmitate to produce jet biofuel over Ni/desilicated meso-Y zeolite catalyst. Fuel 2019;244:472–8.
[38] Zhu Y, Zhang Y, Cheng Z, Guo J, Yang H. Ni-BTC metal-organic framework loaded on MCM-41 to promote hydrodeoxygenation and hydroconversion in jet biofuel production. Int J Hydrogen Energy 2021;46(5):3898–908.
[39] Zanata M, Tri Wulan Amelia S, Mumtazy MR, Kurniawansyah F, Roesyadi A. Synthesis of bio jet fuel from crude palm oil by HEFA (Hydroprocessed Esters and Fatty Acids) using Ni-Mo catalyst supported by rice husk Ash-based SiO2. In Materials Science Forum 2019; 964:193-8. Trans Tech Publications Ltd.
[40] Pires AP, Han Y, Kramlich J, Garcia-Perez M. Chemical composition and fuel properties of alternative jet fuels. Bio Res 2018;13(2):2632–57.
[41] Mullen CA, Boateng AA, Mihalcik DJ, Goldberg NM. Catalytic fast pyrolysis of white oak wood in a bubbling fluidized bed. Energy Fuels 2011;25(11):5444–51.
[42] Van den Bosch S, Schutyser W, Koelewijn S-F, Renders T, Courtin CM, Sels BF. Tuning the lignin oil OH-content with Ru and Pd catalysts during lignin hydrogenolysis on birch wood. Chem Commun 2015;51(67):13158–61.
[43] Jogi R, Mäki-Arvela P, Virtanen P, Kumar N, Hemming J, Smeds A, et al. Biocrude production through hydro-liquefaction of wood biomass in supercritical ethanol using iron silica and iron beta zeolite catalysts. J Chem Technol Biotechnol 2019;94(11):3736–44.
[44] Lindfors C, Mäki-Arvela P, Paturi P, Aho A, Eränen K, Hemming J, et al. Hydrodeoxygenation of isoeugenol over Ni-and Co-supported catalysts. ACS Sustain Chem Eng 2019;7(17):14545–60.
[45] Bomont L, Alda-Onggar M, Fedorov V, Aho A, Peltonen J, Eränen K, et al. Production of cycloalkanes in hydrodeoxygenation of isoeugenol over Pt-and Ir-modified bifunctional catalysts. Eur J Inorg Chem 2018;2018(24):2841–54.
[46] Xing S, Lv P, Wang J, Fu J, Fan P, Yang L, et al. One-step hydroprocessing of fatty acids into renewable aromatic hydrocarbons over Ni/HZSM-5: insights into the major reaction pathways. Phys Chem Chem Phys 2017;19(4):2961–73.
[47] Sonthalia A, Kumar N. Hydroprocessed vegetable oil as a fuel for transportation sector: a review. J Energy Inst 2019;92(1):1–17.
[48] Tirado A, Ancheyta J, Trejo F. Kinetic and reactor modeling of catalytic hydrotreatment of vegetable oils. Energy Fuels 2018;32(7):7245–61.
[49] Wei H, Liu W, Chen X, Yang Q, Li J, Chen H. Renewable bio-jet fuel production for aviation: a review. Fuel 2019;254:115599. https://doi.org/10.1016/j.fuel.2019.06.007.
[50] Vásquez MC, Silva EE, Castillo EF. Hydrotreatment of vegetable oils: a review of the technologies and its developments for jet biofuel production. Biomass Bioenergy 2017;105:197–206.
[51] ASTM. Standard specification for aviation turbine fuels. D1655–19a. West Conshohocken, PA: ASTM International; 2019.
[52] Braun-Unkhoff M, Kathrotia T, Rauch B, Riedel U. CEAS Aeron J 2016;7(1):83–94.
[53] Mandal PC, Abdullah AB, Rahman MM. Total acid number reduction of 2,6-naphthalenedicarboxylic acid using subcritical methanol for reducing acidity of heavy oil: a kinetic study. Proc Eng 2016;148:1213–9.
[54] Jiménez-Cruz F, Laredo GC. Molecular size evaluation of linear and branched paraffins from the gasoline pool by DFT quantum chemical calculations. Fuel 2004;83(16):2183–8.

[55] Gould TD, Lubers AM, Neltner BT, Carrier JV, Weimer AW, Falconer JL, et al. Synthesis of supported Ni catalysts by atomic layer deposition. J Catal 2013;303:9–15.
[56] Li X, Quek X-Y, Michel Ligthart DAJ, Guo M, Zhang Yi, Li C, et al. CO–PROX reactions on copper cerium oxide catalysts prepared by melt infiltration. Appl Catal B Environ 2012;123-124:424–32.
[57] Gan Q, He H, Zhao K, He Z, Liu S. Morphology-dependent electrochemical performance of Ni-1, 3, 5-benzenetricarboxylate metal-organic frameworks as an anode material for Li-ion batteries. J Coll Int Sci 2018;530:127–36.
[58] Yang L, Xing S, Sun H, Miao C, Li M, Lv P, et al. Citric-acid-induced mesoporous SAPO-11 loaded with highly dispersed nickel for enhanced hydroisomerization of oleic acid to iso-alkanes. Fuel Proc Technol 2019;187:52–62.
[59] Zhang Q, Long K, Wang J, Zhang T, Song Z, Lin Q. A novel promoting effect of chelating ligand on the dispersion of Ni species over Ni/SBA-15 catalyst for dry reforming of methane. Int J Hydrogen Energy 2017;42(20):14103–14.
[60] Pu X, Liu N-W, Shi Li. Acid properties and catalysis of USY zeolite with different extra-framework aluminum concentration. Microp Mesop Mat 2015;201:17–23.
[61] Li S, Zheng A, Su Y, Zhang H, Chen L, Yang J, et al. Brønsted/Lewis acid synergy in dealuminated HY zeolite: a combined solid-state NMR and theoretical calculation study. J Am Chem Soc 2007;129(36):11161–71.
[62] Choi M, Cho HS, Srivastava R, Venkatesan C, Choi D-H, Ryoo R. Amphiphilic organosilane-directed synthesis of crystalline zeolite with tunable mesoporosity. Nat Mater 2006;5(9):718–23.
[63] Qiu B, Yi X, Lin L, Fang W, Wan H. The hydroconversion of n-decane over bifunctional Ni-H3PW12O40/SiO2 catalysts. Catal Today 2008;131(1–4):464–71.
[64] Chakraborty R, Das SK. Optimization of biodiesel synthesis from waste frying soybean oil using fish scale-supported Ni catalyst. Ind Eng Chem Res 2012;51(25):8404–14.
[65] Shi Y, Xing E, Xie W, Zhang F, Mu X, Shu X. Enhancing activity without loss of selectivity–Liquid-phase alkylation of benzene with ethylene over MCM-49 zeolites by TEAOH post-synthesis. Appl Catal A Gen 2015;497:135–44.
[66] Du H, Liu D, Li M, Wu P, Yang Y. Effects of the temperature and initial hydrogen pressure on the isomerization reaction in heavy oil slurry-phase hydroconversion. Energy Fuels 2015;29(2):626–33.
[67] Kumar R, Rana BS, Tiwari R, Verma D, Kumar R, Joshi RK, et al. Hydroprocessing of jatropha oil and its mixtures with gas oil. Greem Chem 2010;12(12):2232. https://doi.org/10.1039/c0gc00204f.
[68] Moghadassi A, Amini N, Fadavi O, Bahmani M. Kinetics, thermodynamics and mechanisms for hydroprocessing of renewable oils. Petrol Sci Technol 2011;1:31–7.
[69] Davis BH. Alkane dehydrocyclization mechanism. Catal Today 1999;53(3):443–516.
[70] Morgan T, Grubb D, Santillan-Jimenez E, Crocker M. Conversion of triglycerides to hydrocarbons over supported metal catalysts. Topics Catal 2010;53(11-12):820–9.
[71] Weitkamp J. Catalytic hydroconversion—mechanisms and versatility of the process. ChemCatChem 2012;4(3):292–306.